DYNAMIC ANALYSIS OF A SMALL SCALE BALL MILL STRUCTURE USED FOR GOLD MINING

JUSTIN BYIRINGIRO

MASTER OF SCIENCE

(Mechanical Engineering)

JOMO KENYATTA UNIVERSITY OF AGRICULTURE AND TECHNOLOGY

2019

Dynamic Analysis of a Small Scale Ball Mill Structure used For Gold Mining

Justin Byiringiro

A thesis submitted in partial fulfillment for the degree of

Master of Science in Mechanical Engineering in the

Jomo Kenyatta University of Agriculture and Technology

2019

DECLARATION

This thesis is my original work and has not been presented for a degree in any other university.

Signature..... Date.....

Justin Byiringiro

This thesis has been submitted for examination with our approval as the University Supervisors:

Signature..... Date.....

Dr.-Ing. James K. Kimotho

JKUAT, Kenya

Signature..... Date.....

Eng. Dr. Hiram M. Ndiritu

JKUAT, Kenya

DEDICATION

This work is dedicated to my lovely wife, Mrs Claudine and my daughter Lisper B., for being there for me all through my studies.

ACKNOWLEDGEMENTS

My greatest gratitude goes to the Almighty God and my Savior Jesus Christ for his divine protection and guidance throughout my study.

I'm also grateful to my supervisors, Dr.-Ing. James K. Kimotho and Eng. Dr. Hiram M. Ndiritu for their encouragement, inspiration, and assistance throughout my study period, especially for approaching me as a friend with understanding and patience. I as well thank Professor S.M Maranga, Dr. Onesmus M. Muvengei and Dr. Christiaan Adenya for their continual guidance and encouragement and letting me learn from their experiences during the period of my study. It was a pleasure to have the chance to learn from you. I thank the Rwanda polytechnic (RP) and the Mobility to Enhance Training of Engineering Graduates in Africa (METEGA) for supporting me financially during my study. I also appreciate Mr. Evans Kibiru, Mr. Onyancha, Mr. Mathew N. Kyalo for their special assistance during my research period. My thanks also goes to all my co-Mechanical Engineering postgraduate students, especially Mr. Joseph Kimani, Mr. Philbert Muhayimana, Mr. Peter Mwangi, Mr. Ben Cluade Uwihanganye and Mr. Eugene Gatete, for their assistance.

Finally, thanks to my family, for always backing me at all steps I take.

TABLE OF CONTENTS

LIST OF TABLES

LIST OF FIGURES

LIST OF ABBREVIATIONS

AG	Autogenous
ANSYS	Analysis System
ASM	Artisanal and Small-scale Mining
CAD	Computer Aided Design
DEM	Discrete Element Method
EDEM	Experts in Discrete Element Modeling
FEA	Finite Element Analysis
FE	Finite Element
GDP	Gross Domestic Product
JKUAT	Jomo Kenyatta University of Agriculture and Technology
SAG	Semi-Autogenous
SPH	Smoothed Particle Hydrodynamic
STP	STandard for the Exchange of Product

LIST OF SYMBOLS

C_n	Normal damping coefficient[Ns/m]
C_t	Tangential damping coefficient [kg/s]
$[c]$	Damping matrix
F_n	Normal force [N]
F_t	Tangential force [N]
$F(t)$	Excitation force [N]
f	Frequency [Hz]
g	Acceleration of gravity [m/s^2]
K	Stiffness matrix [N/m]
k_n	Normal contact stiffness [N/m]
k_t	Tangential contact stiffness [N/m]
$[m]$	Mass matrix
N	Critical speed of the ball mill. [rad/s]
R	Radius of the ball mill [mm]
t	Time [s]
u	Nodal displacement [m]
$\dot{u}$	Nodal velocity [m/s]
$\ddot{u}$	Nodal acceleration [m/s^2]
v_n	Normal component of relative velocity[m/s]

v_t	Tangential component of relative velocity $[m/s]$
Δx	Amount of relative approach $[mm]$
μ	Coefficient of friction at the contact $[dimensionless]$
ω	Angular Velocity $[rpm]$
ω^2	Eigenvalue
ω_d	Damped natural frequency
ω_n	Undamped natural frequency
ζ	Damping ratio

LIST OF APPENDICES

ABSTRACT

Ball mills are used as grinding machines in mining, cement, chemical and agricultural industries. They are the most commonly used grinding machines due to their ability to produce fine particles of the material. The communition process, which is the reduction of material to smaller particle size, takes place by abrasion, crushing and impacting through the rotation of the ball mill drum. However, the motion of grinding media upon the rotation of the ball mill causes undesirable vibration in the mill structure which may lead to energy losses, reduction in the performance of the ball mill and fatigue failure of the ball mill structure. Although a lot of research has been conducted to analyze the vibration problem of a ball mill, the tumbling of grinding media charge have not been considered as the excitation load because of the complexity of the dynamics of charges inside the ball mill drum. Therefore the aim of this research work is to analyze the dynamic characteristics of structure of the ball mill developed in JKUAT, by combining Discrete element and Finite element analysis. This is done in order to establish the likelihood of the structure to undergo resonance, and the vibration amplitudes that would result while examining if they are within allowable values based on material and structural properties of the ball mill structure. The ball mill was modeled on Autodesk Inventor 17. The dynamic analysis of the charge inside the ball drum was carried out using Discrete element EDEM software, which resulted in the time varying load applied on the drum. This load was then applied to the FE model using ANSYS software for dynamic analysis of the ball mill structure. Modal analysis was conducted to obtain insight on the possibilities of resonance to occur, by extracting the first ten modes of vibration. Harmonic analysis was conducted to obtain resonance frequencies of the structure. Transient analysis was also conducted and the response of the ball mill structure under time varying load was obtained and compared with the standard limit. Experimental work was carried out and the results were used to validate the FE model which showed a good agreement with a mean error of 5.9 %. It was observed that the ball mill was safe in its range of operation as far as resonance is concerned, as the first natural frequency (7.02 Hz) was far above the operating frequencies (1.67 Hz from the rotation speed and 2.4 Hz from the impact load). The results also showed that the ball mill was subjected to small vibration amplitudes and that the resulting maximum stress was within allowable strength hence would not affect the durability of the ball mill structure.

CHAPTER ONE
INTRODUCTION

1.1 Background

Mining activities carried out using simple machinery and more physical effort are referred to as Artisanal and Small-scale Mining (ASM) (Hentschel, Hruschka, & Priester, 2003). The World Business Council for Sustainable Development (Hentschel et al., 2003) reported that approximately more than 100 million people rely on the mining sector for income especially in developing countries. Mining industries also contribute to the GDP of various countries. Through improving the mining process, Kenya aims to increase the mining sector's contribution to the GDP from 0.8% as of 2015 to 10% by 2030 (Barreto, 2018). Although large-scale mining (LSM) companies have operations in Kenya, Artisanal and small-scale mining (ASM) remains a significant activity. For instance in 2015, LSM employed around 9,000 workers whereas ASM was estimated to employ 146,000 people (Seccatore, Veiga, Origliasso, Marin, & Tomi, 2014). In 2013, the total gold production was approximately 3.6 tonnes. Artisanal and small scale gold mining produces about 5 tonnes per year. In the communition process, ASM uses minimal machinery, simple techniques and more physical effort. Improving communition process of artisanal and small–scale mining is highly needed. In Kenya, ASM miners are found in Narok County, Kakamega County and Migori County. To improve how the of grinding gold is done, a small scale ball mill is being developed in Jomo Kenyatta University of Agriculture and Technology (JKUAT). This ball mill needs to be well designed and optimized in order to maintain its integrity and usefulness hence the motivation for this study.

1.2 Ball mill

A ball mill is the tumbling grinding machine most commonly used in mineral processing industries. It is a versatile grinding mill and has a wide range of application. Particle breakage in a ball mill takes place by impact, friction and abrasion between rocks and steel balls inside the mill during rotation. The steel balls are charged into a drum, along with the material to be ground and rotated, allowing the balls to crush the material that travels between them. A ball mill is composed mainly of a drum, motor, power transmission mechanism and the frame support as shown in Figure 1.1. Detailed parts are shown in Appendix I.

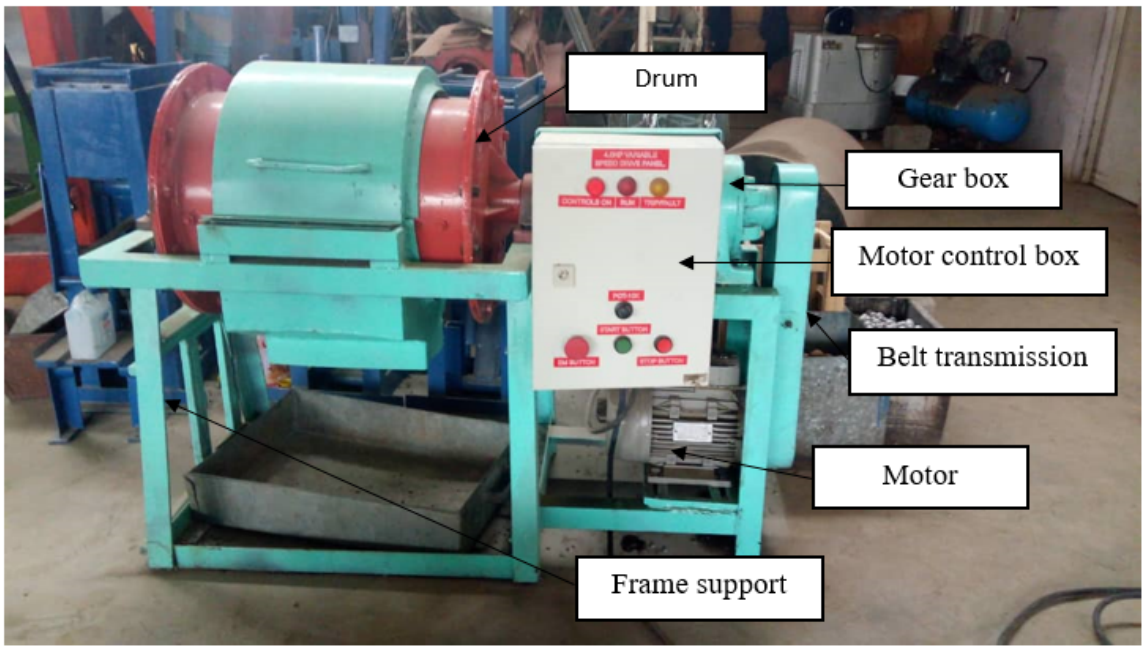

]p78i
m

Figure 1.1: Main parts of the ball mill developed in JKUAT

1.2.1 Vibration in a ball mill

Vibration in ball mills can be a serious problem that could lead to failure of the structural components. In addition, vibration is accompanied by energy losses and reduction in performance that result in higher operating cost of the ball mill. Beside the basic vibration from the rotary drum and machine assembly (caused by imbalance, misalignment, eccentricity of rotating drum, gears, keys and keyways in shafts, damages and faults in bearings, looseness of machine elements etc.), the tumbling of steel balls and the charge are the main vibration sources (T. Q. Li et al., 2015), (Francisco, Joaqu Manuel, aguado Juan, & d Juan, 2018). Figure 1.2, shows the causes of ball mill drum vibrations (Tang, Wu, & Liu, 2016).

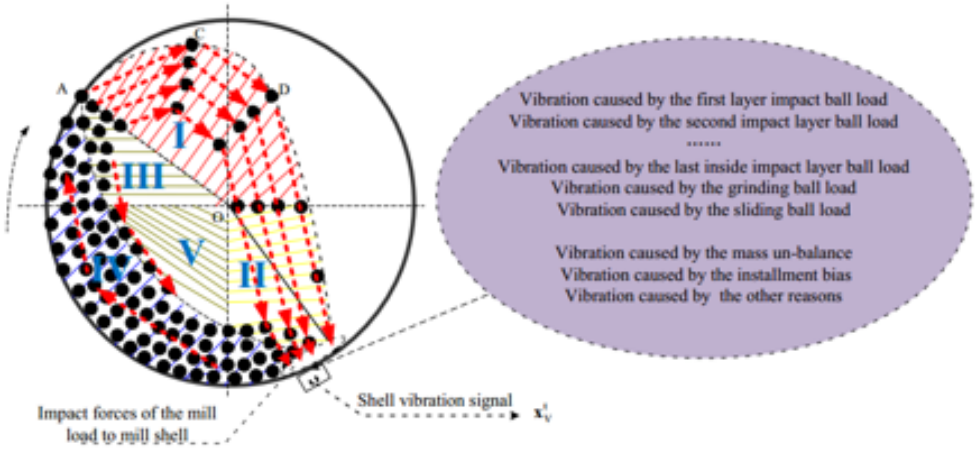

Figure 1.2: Causes of mill drum vibrations (Tang et al., 2016)

High dynamic forces are present during the operation of a ball mill. The entire load is transferred to the supporting structure during operation. There are a lot of examples of failures caused by unpredictable dynamic loads (Rusinski, Czmochowski, Iluk, & Kowalczyk, 2010), (Rusinski, Dragan, Moczko, & Pietrusiak, 2012). (Rusiński, Moczko, Pietrusiak, & Przybyłek, 2013) observed a number of cracks on the supporting structure a few weeks after starting the operations, caused by poor design of the structure. It is therefore important to effectively design a ball mill so that such a vibration problem does not occur. It is also essential for the profitability of mining operations that the ball mill can run continuously with minimal time set aside for maintenance.

1.2.2 Motion of the charge in a ball mill

The ball mill drum is filled with steel balls of various sizes. The material which is being ground together with steel balls is called the mill charge. Due to the rotation and friction of the mill drum, a kidney-shaped cross section grinding path is formed at the rising side of the drum. Grinding media that reach the top of that kidney (position of dynamic equilibrium), fall down impacting on other grinding media as illustrated in Figure 1.3.

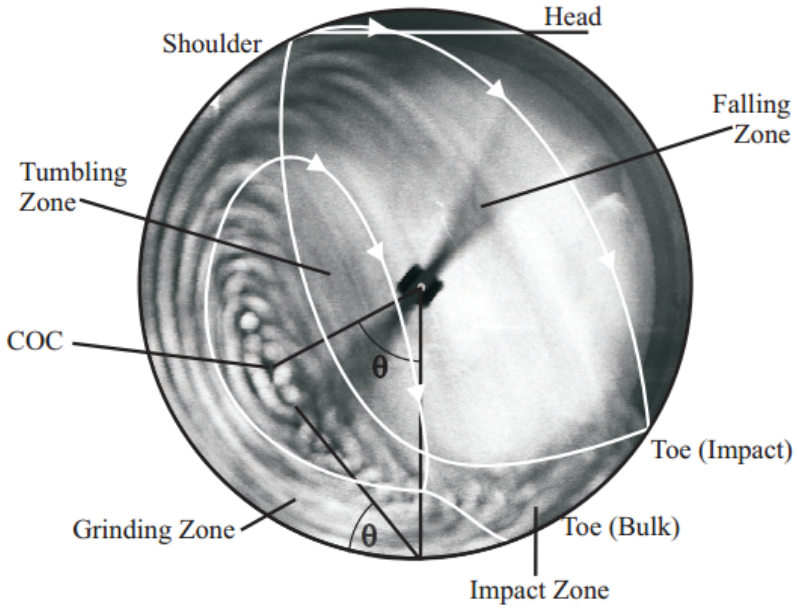

Figure 1.3: Charge motion (Martins, 2011)

It is difficult to describe the tumbling action accurately and it is complicated to calculate the motion of an individual ball during rotation of charge (King, 2001). At lower speeds the impact motion produces mechanical vibration of low intensity. However, as the speed increases, the number of impacts of balls increase and through it, the intensity of vibration of the ball mill also increases (Rahmanovic, Lukavac, Isic, & Mostar, 2008).

1.3 Problem Statement

A ball mill is more preferable than other grinding machines (Rod mills, Stirred mills etc). Grinding in a ball mill takes place by impact, friction, and abrasion between rocks and steel balls inside the mill during rotation. However, tumbling of balls and material to be ground causes inevitable vibrations in a ball mill during its operation. These vibrations are then transferred to the supporting structure of the ball mill Which may lead to resonance when any of the natural frequencies match with the operating frequency of the mill. In addition, these vibrations may cause fatigue and failure of the structural components if the amplitudes of vibrations are out of the allowable range. Moreover, the vibration is accompanied by energy losses and reduction in performance of the ball mill. Although a lot of work has been done on dynamic analysis of the ball mill using finite element

analysis, the tumbling of grinding media charge has not been considered as the excitation force to the ball mill supporting structure. This is due to the complexity of the dynamic of charges inside the ball mill drum. Impact forces inside the ball mill drum resulting from the tumbling of grinding media can be estimated using discrete element method, and the dynamics of the charge inside the drum can be easily studied from here(Jian Tang & Liu, 2016). In this study a combined discrete element and finite element model was developed to predict resonance possibilities and to analyze the severity of vibration.

1.4 Objectives

The main objective of this study was to analyze the dynamics of structural components of a small scale ball mill. The above objective was achieved via the following specific objectives:

1. To model the ball mill structure and carry out discrete element analysis in order to obtain the excitation forces from impact of tumbling of charge and steel media.
2. To carry out modal and harmonic analysis in order to know the possibilities of resonance in the ball mill structure.
3. To carry out transient analysis in order to study the severity of vibration in ball mill structure.
4. To conduct a vibration experiment of the ball mill in order to validate the finite element results.

1.5 Justification

Size reduction is one of the most fundamental operations in the mineral processing industry. A ball mill is one of the most preferred in the gold processing industry because of its fine finishing. The primary purpose of size reduction is to obtain an appropriate product size with least possible energy consumption (Petrakis, Stamboliadis, & Komnitsas, 2017). Nevertheless, size reduction is accompanied with vibration which causes energy losses, reduction in the performance and high power consumption, as consequence of that, the operating cost of the ball mill becomes higher. The vibration may even lead to failure of the structure of ball mill. This study contributes to the development of artisanal and small scale mining (SAM) in Kenya and neighboring countries, by providing a safe ball mill as far as vibration is concerned.

1.6 Thesis Structure

This thesis is divided into five chapters as follows: Chapter 1 gives an introduction, overview of the ball mill. Chapter 2 contains the literature review. Research work that have been carried out are reviewed. Chapter 3 contains Methodology, procedures used to obtain the data for the research. Chapter 4 contains results and discussion. the outcomes from simulation are presented and discussed and compared with experimental results. Chapter 5 has the conclusions relating to the present work and recommendations of the possible improvements and future work.

CHAPTER TWO
LITERATURE REVIEW

2.1 Overview

This chapter presents a review of the research work that has been carried out concerning the ball mill, mainly focusing on the structural vibration. A review of FEM and DEM and effect of parameters on vibration of the ball mill are also presented in this chapter.

2.2 Mineral Processing

Ores extracted from the earth contain valuable minerals and gangue. The minerals must be liberated from the gangue and this is achieved by crushing and grinding processes called communition. The valuable minerals are processed while the gangue are considered waste. Figure 2.1 shows the stages in mineral processing. The extracted ore is first crushed then ground to produce fine particles. After separation, valuable minerals are further processed and gangue are disposed.

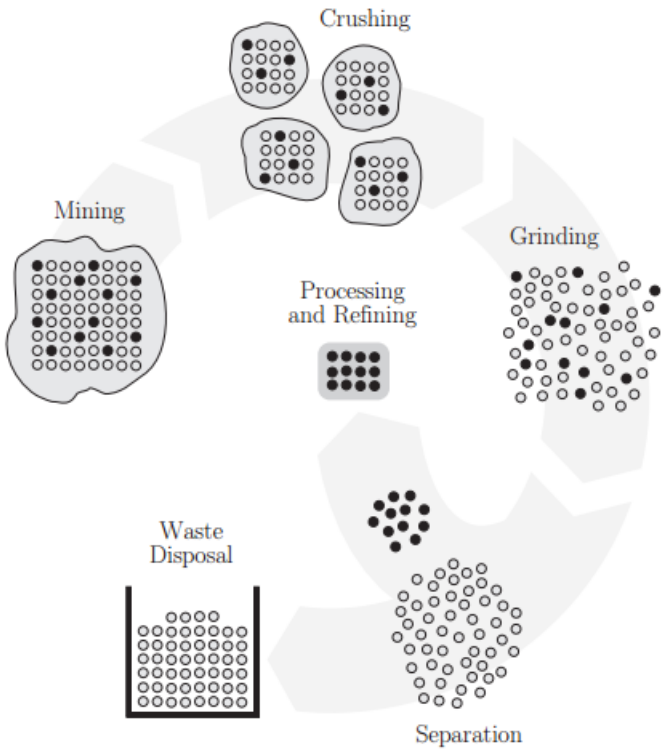

Figure 2.1: Stages in mineral processing (Fuerstenau & Han, 2003)

2.2.1 Communition

Communition is the process of breaking material of a given particle size to a smaller particle size by the application of large stress. In mineral processing, particles containing valuable minerals must be broken in order to liberate these valuable minerals. The process involves both crushing and grinding (Wills & Napier-munn, 2006). The communition process is illustrated in Figure 2.2.

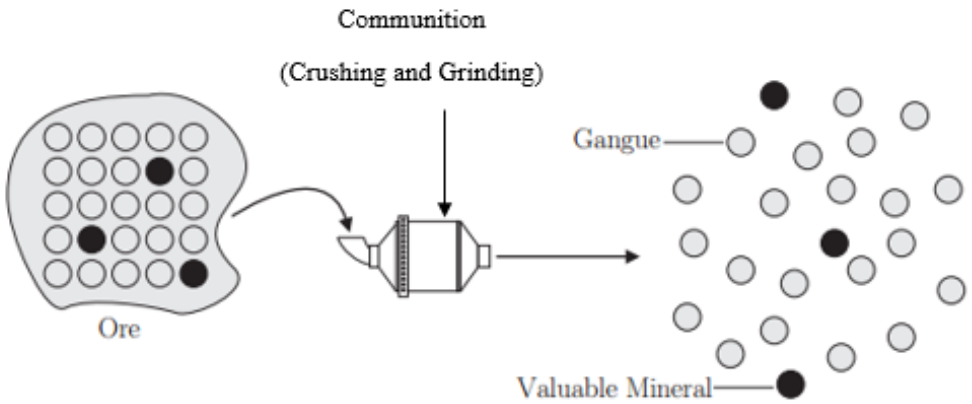

Figure 2.2: Communition process (Martins, 2011)

2.2.2 Communition Machines

There exists a number of communition machines used in mineral processing. They are classified depending on the size of the ore they process. Generally, communition machines are classified within two groups: Crushers and grinders (Wills & Napier-munn, 2006). Figure 2.3 lists some communition machines.

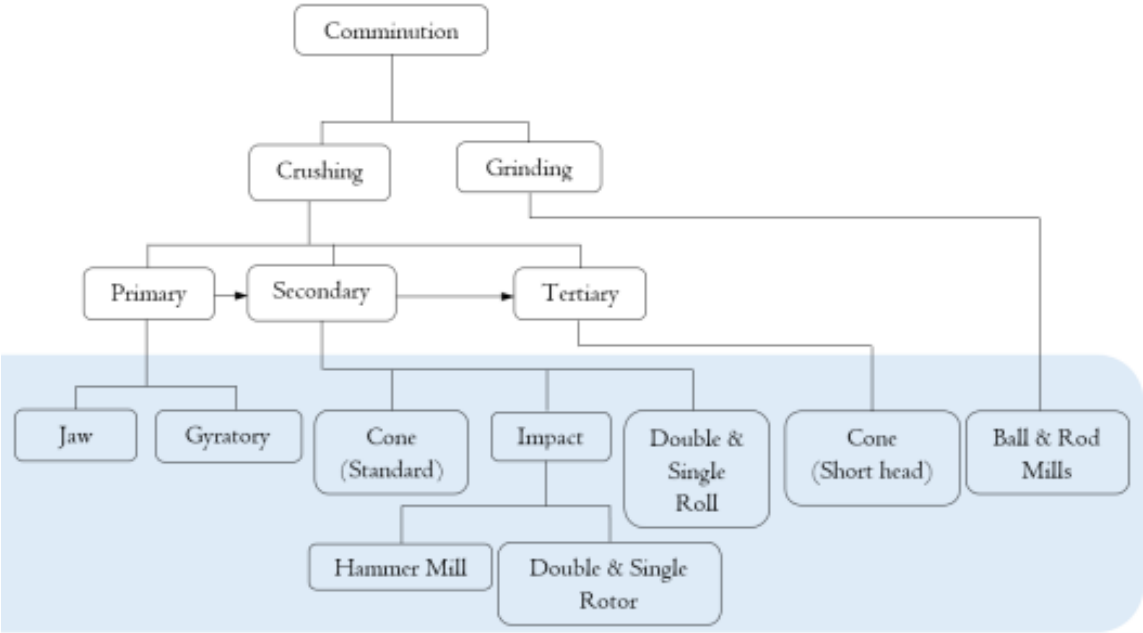

Figure 2.3: Communition machines (Kalemtas, 2013)

2.2.2.1 Crushing

Crushers are used during the early stages of mineral processing. This type of machine is applied to ores large than $10^4 \mu$m, and reduces the size of the ore by impact and compression. This class of communition machines includes compression rollers, jaw crushers, hammer mills and cone crushers (Wills & Napier-munn, 2006).

2.2.2.2 Grinding

Grinding is the second step of mineral processing and the last stage of the communition process. Grinding is performed in a rotating cylindrical vessel which contains crushed ore and grinding medium (usually balls made of steel), free to move inside the mill. Due to the rotation of the drum, the charge is lifted and tumbles onto the drum wall causing the breaking of ore by impact and attrition. Grinding takes place through several mechanisms, including impact or compression due to forces applied almost normally to the particle surface chipping due to oblique forces; and abrasion due to forces acting parallel to the surfaces. These mechanisms distort the particles and change their shape beyond their elastic limit, causing particles to break.

Depending on how the motion is imparted to the charge, grinding mills are generally classified into three types: tumbling mills, stirred mills, and vibrating mills as shown in Figure 2.4. Vibrating mills have a filled grinding chamber which vibrates by cams or unbalanced weights. They are new grinding mills and less common. In stirred mills, the mill drum (horizontal or vertical) is stationary and the motion is transmitted to the charge by the movement of internal stirrer. The stirred mills are used for fine grinding of soft materials. Tumbling mills are commonly used in mineral processing.

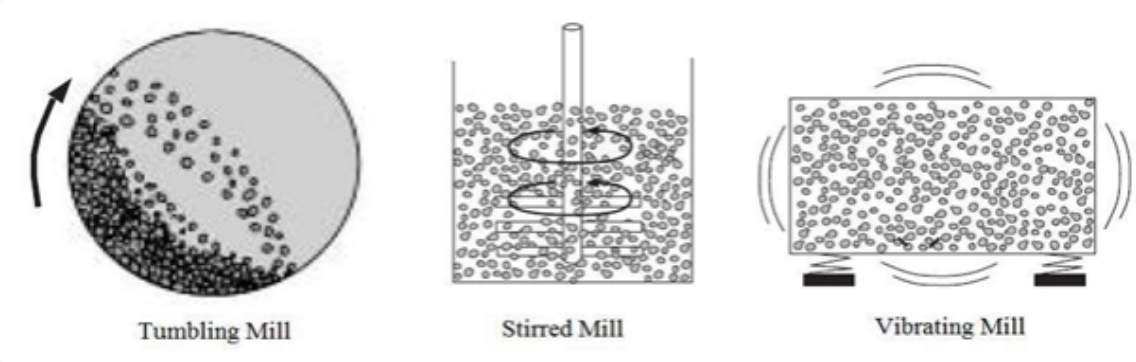

Figure 2.4: Types of grinding machines (Wills & Napier-munn, 2006)

2.2.2.3 Tumbling mills

In tumbling mill, the mill drum is rotated and motion is imparted to the charge via the drum. The grinding medium may be steel rods, steel balls, or rock itself. Tumbling mills are typically employed in the mineral industry for coarse-grinding processes, in which particles between 5 mm and 250 mm are reduced in size to between 40 and 300 μm. Figure 2.5 shows the mechanism of grinding in tumbling mills.

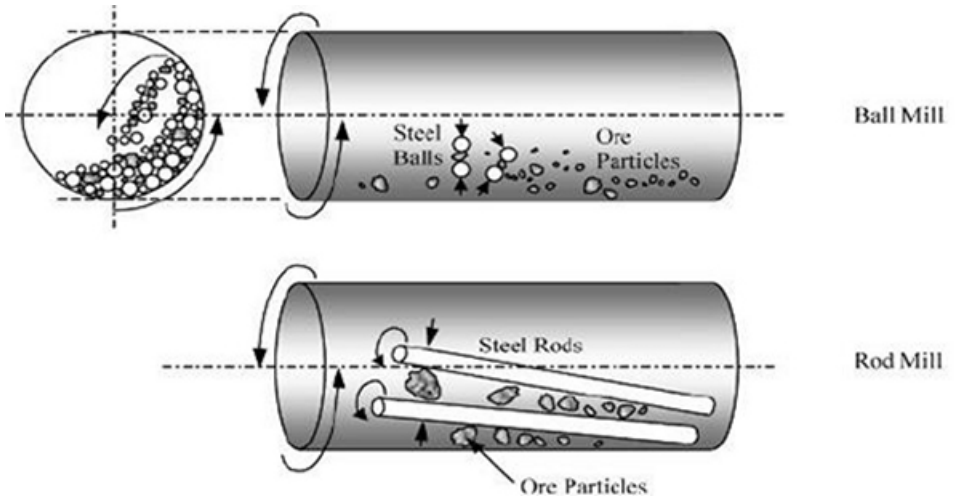

Figure 2.5: Grinding in tumbling mills (Wills & Napier-munn, 2006)

Tumbling mills are classified into:

1. Rod mills : uses rods as the grinding medium
2. Ball mills: uses steel balls as the grinding medium
3. Autogenous (AG) Mills : self grinding of the ore
4. Semi-Autogenous (SAG) Mills : similar to AG mills, difference lies with the addition of a small quantity of grinding balls to aid grinding just like ball mills.

Mills can operate either in a batch mode or a continuous mode. In the batch mode, a fixed quantity of charge is ground and subsequently discharged. When filling or discharging, the mill must be stopped. In the continuous mode, the charge added to the mill at the feed, is ground and exits at the discharge without stopping the operation of the mill.

2.3 Critical speed of a ball mill

The Critical Speed for a grinding mill is defined as the rotational speed where centrifugal forces equal gravitational forces at the mill drum's inside surface. This is the minimum rotational speed where grinding media will not fall away. It is the speed where the weight of the grinding charges is balanced by the centrifugal force, as illustrated in Figure 2.6 (Toram, 2005). The critical speed is obtained from the Equation 4.2 or 2.4.

$$mN^2R = mg, \tag{2.1}$$

$$N = \sqrt{\frac{g}{R}}, \tag{2.2}$$

where, N is the critical speed, g is acceleration of gravity, R is the radius of ball mill. The critical speed is usually expressed in terms of revolutions per second.

$$N = \frac{1}{2\pi}\left(\sqrt{\frac{g}{D}}\right) = \frac{\sqrt{2\times 9.81}}{2\pi\sqrt{D}} = \frac{0.705}{\sqrt{D}}, \tag{2.3}$$

Equation 4.2 becomes;

$$N = \frac{42.3}{D^{0.5}}, \tag{2.4}$$

where, D is the ball mill diameter and N is the critical speed in rpm

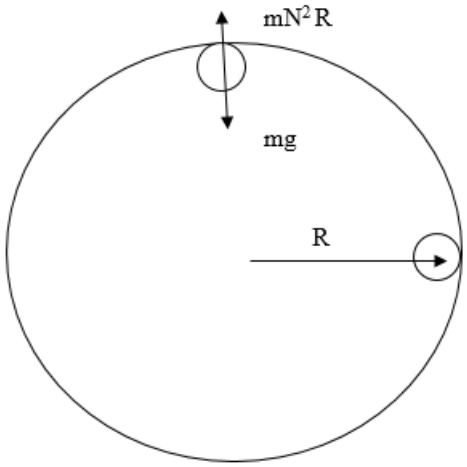

Figure 2.6: Centrifuging condition (Toram, 2005)

2.4 Analysis of Vibration in a Ball Mill

(Rahmanovic et al., 2008), investigated the vibration of a ball mill under variable load. Due to the production requirements, the capacity of the ball mill was variable and therefore the measurement of vibration was done for two different capacities. Vibrations signature showed different vibration levels at different loads. It was found that there is correlation between the load and the intensity of vibration of the ball mill components because the amplitudes of vibration at the same frequencies decrease with increase of load in the ball mill.

(Mayur & Vishal, 2014) designed a ball mill for paint industries, the aim was to optimize structural parameters. Optimization was done by modeling and analyzing of parts of ball mill by using Finite element method, ANSYS 14.0. It was found that as the mill thickness decreased, Von Mises stress and deformation increased. However, in this research the impact load on the ball mill during rotation was not taken into account.

(Palsson & Jonsén, 2009) conducted research where DEM and FEM were used together to model a tumbling mill. DEM was used to model the charge and FEM to model the mill structure. The aim was to predict contact forces for varying mill dimensions. During the rotation of the mill drum, charge-charge and charge-structure interactions occurred in the mill system. The contact between charge particles and structure of the mill resulted in load

to the structure of the mill. The structure of the mill deformed due to the load from the charge. Because of this deformation there were rises of strains and stresses in the structure of the mill. However, only the ball mill drum was considered and the focus of authors was not to analyze the vibrations of the structure.

(Jonsen, Bertil, & Haggblad, 2011), used the smoothed particle hydrodynamic (SPH) method together with finite element method (FEM) to model the same tumbling mill in (Palsson & Jonsén, 2009). The goal of the research was to model the physical interaction between charge and mill structure. The results from these two approaches were the same except that the latter gave more information on the drum response and its influence on the charge motion. In both cases the results were validated using experimental data. However, only the ball mill drum was considered.

In the research done by (Liu, 2008), finite element model of the ball mill cylinder was developed to investigate the impact excitation effect on the vibration behavior. It was found that the maximum magnitude of structural vibration appears on the mid of cylinder. However, in this research, the model was only of the ball mill shell and the rotation speed was the only considered excitation frequency.

(Toram, 2005) Investigated the effect of grinding media oscillation on torsional vibrations in tumble mills using Lab VIEW Torsion. It was observed that there is big correlation between the torsional vibration and the oscillation of grinding media. (Petrakis et al., 2017) explored the grinding of quarts in a ball mill using population balance modeling, in order to identify the optimal mill operating parameters. However, the aim of this work was the process inside the ball mill drum not the structure.

2.5 Resonance in Ball Mills

Resonance is a condition that occurs in mechanical structures and can be described as sensitivity to a certain vibration frequency. Resonance occurs when a natural frequency is at or close to a forcing frequency (Ahmed, 1991). When present, this condition can cause severe vibration levels by amplifying small vibratory forces from machine operation. In order to avoid the resonance, natural frequencies and mode shapes must be calculated and analyzed through modal analysis. Since any dynamic response of a structure can be obtained as a combination of its modes, a knowledge of mode shapes, modal frequencies and modal damping ratios constitutes a complete dynamic description of the structure (Rao, 2010). In a ball mill, resonance occur if any of the natural frequencies of the ball

mill structure happen to match either the frequency resulting from the operating speed of the ball mill or the excitation frequency resulting from the tumbling of charge. In a case study by (Radziszewski, Quan, & Poirier, 2017), Resonance problem was suspected in an operating ball mill. The effect of parameters on vibration was explored and it was found that the reason behind failure was the natural frequency matched with the operating frequency of the ball mill. This problem was addressed by adding extra mass to the mill drum, the mills' natural frequency was lowered out of the operating range. However, this solution affected the power consumption negatively. (Chen, Xue, Liu, & Li, 2014) used ANSYS workbench, to carry out modal analysis of an oversize ball mill tube to analyze the possibilities of resonance. The first ten natural frequencies were calculated since the lowest order modes have a huge impact on vibration (Hao, Yong-jun, & Xiao-ping, 2016). It was found that resonance would not happen since the operating frequency of ball mill tube was 0.26 Hz, and the lower natural frequency of mill tube from the modal analysis was 16.816 Hz, which was much higher than the operating frequency. In addition, it was found that the maximum amplitude occurred in the middle of the drum and hence the crack would happen in the drum much easier than in other area. However, this study considered only the ball mill drum and the aim of the study was only to carry out a modal analysis and to give a reference to the designers of the ball mill. (Quan, 2006) explored the tumbling mill's resonance using six different kinds of mill FE models. Modal analysis was performed to compute natural frequencies and corresponding modes shapes in order to investigate resonance behavior. However, in order to simplify the simulation, only the mill drum was considered while the other parts of the mill system were not taken into consideration. (Porto, Carvalho, & Mendonca, 2012) used Finite Element Method to analyze the natural frequencies of the base of the ball mill. It was found that there was no risk of resonance since these frequencies were outside the limits of the operating frequency. However the finite element model in this study considered only the base of the ball mill. (Wojcicki, Grosel, Sawicki, & Majcher, 2015) carried out modal analysis of the ball mill foundation. Finite element method was used to model and results were validated using experimental investigation. It was found that the poor condition of the ball mill was caused by the excessive vibration.

2.6 Ball mill Parameters that affect vibration

The vibration of the ball mill is affected by the stiffness of structure of the ball mill, and its mass since the natural frequency is dictated by those two parameters. For example adding

extra mass to the mill will effectively lower its the natural frequency(Radziszewski et al., 2017). The transmitted load from the ball mill drum to the frame support, The thickness of the shaft can also affect the vibration of a ball mill (Mayur & Vishal, 2014), since the whirling motion of shafts causes the center of gravity of a shaft cross section to move in an elliptical orbit around the center of rotation (Quan, 2006). (Zeng & Forssberg, 1992) carried out experiments on a laboratory scale ball mill to analyze the correlation between the vibration and the operating parameters of the ball mill. It was found that the mill speed and the filling level have effect on the vibration signal. As the mill rotation speed increased the vibration signal was increasing and the vibration signal was decreasing as filling level decrease.

2.7 Finite Element Method

The finite element method (FEM) is a numerical method for solving problems of engineering and mathematical physics. FEM is useful for problems where analytical solution cannot be obtained because of the complicated geometries. FEM allows visualization of where structures bend or deformed, and shows the distribution of stresses and displacements (Moveni, 2009). FEM reduces problem to that of a finite number of unknowns by dividing the domain into elements and by expressing the unknown field variable in terms of the assumed approximating functions within each element, as illustrated in Figure 2.7.

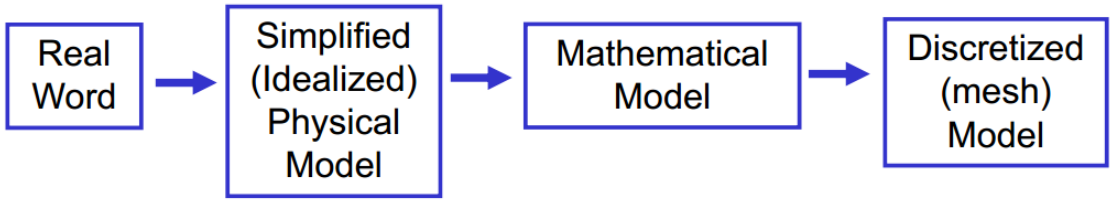

Figure 2.7: Discretization of problem (Moaveni, 1999)

2.7.1 Finite element Software

There are enormous number of software packages that implement the Finite element method for solving problems. The most common ones include: Abaqus, HyperMesh, ANSYS, LS-DYNA, etc. In this research work ANSYS was used to carry out vibration analysis of a ball mill, because of its capabilities in structural dynamics (Erke Wang, 2002). ANSYS is one of the leading commercial finite element programs and can be

applied to a large number of applications in engineering. The ANSYS user is able to run simulations for linear and nonlinear problems in engineering where structural nonlinearities may occur due to nonlinear material behaviour, large deformations or contact boundary conditions.

ANSYS software solve the equation 2.5

$$[m]\{\ddot{u}\} + [c]\{\dot{u}\} + [K]\{u\} = \{F(t)\}, \tag{2.5}$$

where $[m]$ is mass Matrix, $[c]$ is damping matrix, $[K]$ is stiffness matrix, $\{\dot{u}\}$ is nodal velocity, $\{\ddot{u}\}$ is nodal acceleration, $\{u\}$ is nodal displacement, $\{F(t)\}$ is the excitation Force.

Different dynamic analysis (Modal, harmonic and transient analyses) can be done in ANSYS. Modal analysis determines the fundamental vibration mode shapes and their frequencies (James, Smith, Wolford, & Whaley, 1994). ANSYS provides different eigenvalue solvers for modal analysis designed for special application purposes. Example of eigensolvers provided by ANSYS include; Block lanczos method, Subspace method, Reduced method and Powerdynamics method. The Block Lanczos method is a very efficient algorithm to perform a modal analysis. In addition its convergence rate is much higher compared to other extraction method (W. Li, Pu, Liu, Chen, & Zhang, 2009; Bathe, 2016). Harmonic analysis is helpful in verifying whether or not the structure of the ball mill will successfully overcome resonance and harmful effects of forced vibrations ("ANSYS Mechanical, Harmonic Response", 2009). Though from modal analysis the possibility of a structure to be subjected to resonance can be known, harmonic analysis is also needed to detect resonant response and to avoid it if necessary (Yu, Zhang, Li, Wang, & Tang, 2017).

The right hand side of Equation 2.5 becomes:

$$F = F_0 cos(\omega t) \tag{2.6}$$

Equation 3.1 becomes;

$$m\ddot{x} + c\dot{x} + kx = F_0 cos(\omega t) \tag{2.7}$$

The vibration amplitude is defined by the Equation 2.8.

$$X = \frac{F_0}{k} \frac{1}{\sqrt{(1-r^2)^2 + (2\zeta r)^2}} \tag{2.8}$$

where, X is the amplitude of vibration, k is the stiffness, r is the ratio of the force frequency over the undamped natural frequency, ζ is the damping ratio. ANSYS workbench solve equation 2.8 and plots the frequency response which shows the resonant frequency of the system. For transient analysis, ANSYS provides different solution options such as Full method, Reduced method and Mode Superposition method. The Full method is simple to use since it does not reduce the dimension of the considered problem. A technique used for discretization of the problem is called meshing. Three types of element can be used in meshing. Tetrahedral, hexahedral and polyhedral element, the later is for CFD analysis. Advantages of hexahedral over tetrahedral is that hexahedral is faster with better accuracy ("ANSYS Meshing Advanced Techniques", 2017).

2.7.1.1 Merits of ANSYS

(i) ANSYS can handle very complex geometries.

(ii) ANSYS can handle a wide variety of engineering problems.

(iii) Robust collection of meshing algorithms.

(iv) ANSYS can handle complex loading.

(v) Easily integrated with CAD packages for complex geometries.

2.7.1.2 Demerits of ANSYS

(i) Only approximate solutions are obtained.

(ii) Less control of mesh specifics, structured meshing more difficult.

(iii) Ansys software has inherent errors.

2.8 Discrete Element Method

The discrete element method (DEM), is a numerical modeling method used for computing the motion and collision of particles (B. Mishra & Rajamani, 1992). It is a method that tracks the motion of individual particles based on equations of motion. Discrete el-

ement method is applied to many fields including; granular flows, traffic and crowd dynamics, astronomy, computer networks, biosystem interactions, agriculture, pharmaceuticals and mineral processing (Wassgren & Sarkar, 2008; Cleary, 1998; Weerasekara et al., 2013).

DEM provides a calculation cycle which solves the dynamic interaction of particles. The main stages are: contact detection, calculation of contact forces and numerical time integration. Figure 2.8 shows the DEM process.

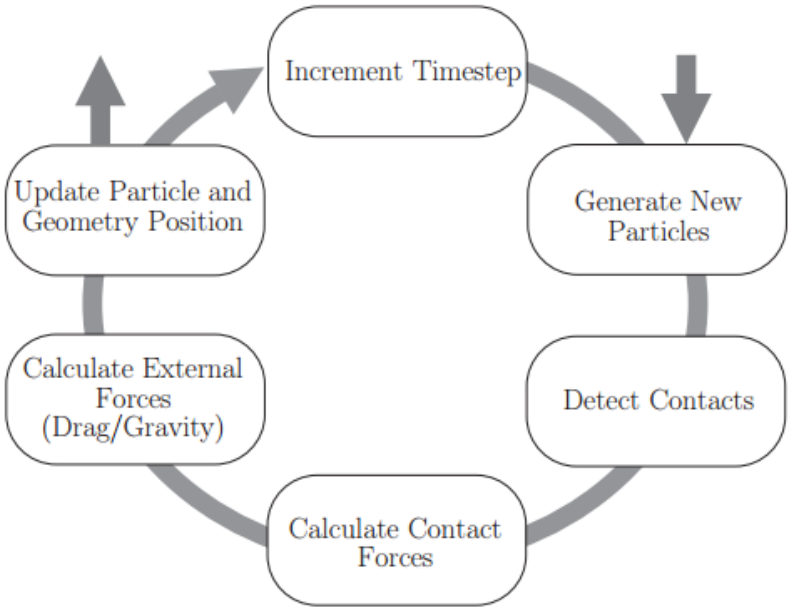

Figure 2.8: DEM simulation process (Martins, 2011)

New particles and geometry are created, consisting of solid bodies that are necessary to the simulation. Force-displacement laws included within contact models, determine internal forces resulting from element interactions. Based on the external forces, Newton's second low of motion is used to provide acceleration for each particle. The position of each particle and contacts are updated, the calculation cycle continues until when a specified number have been completed. One of the software that can carry out Discrete element method is EDEM. EDEM is a DEM simulation software property of DEM Solutions Ltd.,UK, which is used in the simulation and analysis of particle handling and processing operations ("EDEM 2.4 User Guide", 2011). EDEM is a commercial code that includes a powerful Graphical User Interface (GUI) that interfaces with CAD drawing softwares.

2.8.1 Application of DEM to Communition

When applied to communition, discrete element method gives an opportunity to study several aspects of grinding such as; size distribution, collision forces, energy loss, power consumption, etc. (Venugopal & Rajamani, 2001) analyzed the motion in tumbling mills using discrete element modeling. A simple spring -damper collision model was used in simulation. The results were validated using experimental results and showed good agreement. However, the study focused only on the process inside the drum without considering the structure. (Francisco et al., 2018) explored the possibility of using DEM to characterize the load torque of tumbling ball mills using DEM simulations and experimental tests on a pilot scale ball mill. It was shown that due to the operating principle of ball mills, the load appearing in a tumbling ball mill was time varying.

2.8.2 Contact Models

Several contact models are available in discrete element analysis to describe the interaction between particles. These models include:

1. Linear-spring damper model
2. Nonlinear-spring dashpot model.
3. The elastic perfectly plastic contact model.

The discrete element method used for comminution modeling generally use a linear spring and dashpot model in both the normal and tangential direction (Weerasekara et al., 2013). Linear contact is the simplest contact in which the spring stiffness is constant. It is suited to tracking the motion and gross kinetics of a large number of particles (Venugopal & Rajamani, 2001). Figure 2.9 shows the collision force using linear contact. In a ball mill, the collision between sphere to sphere and sphere to wall of the drum are modeled in a similar way (Venugopal & Rajamani, 2001).

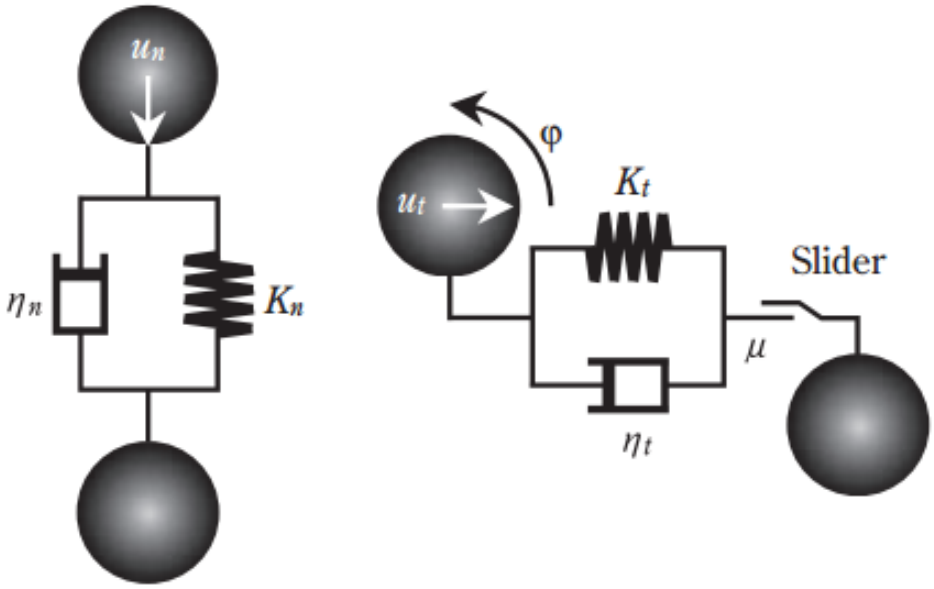

Figure 2.9: Normal and shear force during collision (Sheng-yong et al., 2012).

The contact force of steel ball has two components, normal and tangential as shown in Figure 2.9. The equation for calculating the contact forces are shown in Equation 2.11 and 2.14 (Venugopal & Rajamani, 2001; B. K. Mishra, 2003).

2.8.2.1 Normal Force

The normal contact force is described as

$$F_n = k_n \Delta x + C_n v_n, \tag{2.9}$$

where k_n is the normal contact stiffness, v_n is the normal component of the relative velocity of the particles, C_n is the damping coefficient and Δx is the amount of relative approach. The magnitude of the normal force is updated at every time step and the value of the contact force at time t + Δt is calculated from its value at time t as:

$$F_n(t + \Delta t) = F_n - k_n v_n \Delta t, \tag{2.10}$$

where F_n is the normal force at the end of the previous time step. Introducing contact

damping, Equation 2.10 becomes;

$$F_n(t+\Delta t) = F_n - v_n k_n \Delta t + C_n v_n, \tag{2.11}$$

where C_n is the normal damping coefficient.

$$C_n = -2\ln(e)\left(\sqrt{\frac{k_n m}{\ln^2 e + \pi}}\right), \tag{2.12}$$

where k_n is the normal contact stiffness, m is the normalized mass, and e is the coefficient of restitution.

2.8.2.2 Tangential Force

The magnitude of the tangential force is

$$F_t = min\left\{\mu F_n, k_t \Delta_t + C_t V_t\right\}, \tag{2.13}$$

where μ is the coefficient of friction at the contact, F_n is the Normal force, k_t is the tangential contact stiffness, Δ_t is the amount of relative approach, C_t is the damping coefficient and v_t is the tangential component of the relative velocity of the particles. The magnitude of the tangential force must be updated also at each time step.

$$F_s(t+\Delta t) = F_t - v_t k_t \Delta t, \tag{2.14}$$

where F_t is the tangential force at the end of the previous time step, k_t is the tangential contact stiffness and v_t is the tangential component of the relative velocity of the particles.

2.9 Linking EDEM to ANSYS

Forces acting on the ball mill drum from the tumbling of media are linked to ANSYS analysis to be used as an input loading condition condition for FEA simulation. Simulation of the ball motion within the ball mill using EDEM, helps to understand the impact forces of the balls to the mill shell. The resulting forces from EDEM are exported to ANSYS to serve as the source of excitation to the ball mill. ANSYS is then used to obtain the response of the ball mill to these excitations. (Tang et al., 2016) analyzed vibration signal

of the ball mill shell based on DEM-FEM method, where a ball mill drum model was exported to EDEM for producing impact forces then these forces were added on FEM model of the ball drum for analysis. However, the aim of this study was to construct a sensor and frame support was not included in the model. (Jons Pson, Tano, & Berggren, 2011) used a combined DEM-FEM model to study the interaction between the charge and the mill structure. It was possible to accurately predict the occurrence and patterns of mechanical waves traveling in the mill shell and lining. The output from EDEM software can also be extracted ("EDEM 2.4 User Guide", 2011) and inserted to ANSYS workbench using tubular method (Moveni, 2009). The right side of Equation of motion 3.1, becomes the forces in Equation 2.10 and 2.14.

2.10 Summary

This chapter has covered what researchers have done on the ball mill in terms of vibration analysis, and how the vibration problems were addressed. The researches which have been conducted, have not been able to solve efficiently the vibration problems in a ball mill structure. The following gaps were identified from the literature reviewed:

1. Most of research considered only the ball mill drum during analysis. Since it has been shown that the vibration from the ball drum is transferred to the structure, there is a need to analysis the support structure of a ball mill.

2. Modal analysis have been the only dynamic analysis conducted, because the focus of some research was only the resonance. Therefore, there is a need to conduct more detailed dynamic analysis, to evaluate amplitudes of vibration that can cause the harmful effects during the operation of a ball mill.

3. Though the excitation force from the tumbling media has been considered by some researchers to analyzing ball mill drum, it was ignored when analyzing the frame support because the motion inside the drum is complex which make it difficult to know the dynamics of the charge. Since it has been established that the main cause of vibration is the tumbling of charge, there is a need to conduct analysis of the frame taking into account the excitation force resulting from tumbling of the charge.

This research is aimed at addressing all these identified gaps.

CHAPTER THREE
METHODOLOGY

3.1 Introduction

The aim of this research work was to conduct vibration analysis of a small scale ball mill for gold mining, by studying its dynamic characteristics under time varying load subjected to its structure during operation. Figure 3.1 illustrates the method used in this research work. At first two models, one of ball mill drum only and another of ball mill structure with the frame support, were developed using Autodesk Inventor 2017 CAD software. The first model was exported to EDEM software for discrete element analysis which resulted in time varying load, which was used as the excitation force on the drum. The second model was exported to Ansys Workbench for structural analysis using FEM, where modal, harmonic and transient analysis was performed. After obtaining simulation results, validation was done by carrying out experimental tests on the ball mill developed in JKUAT. This chapter therefore, presents detailed procedure used in modeling the ball mill structure and steps used in vibration analysis.

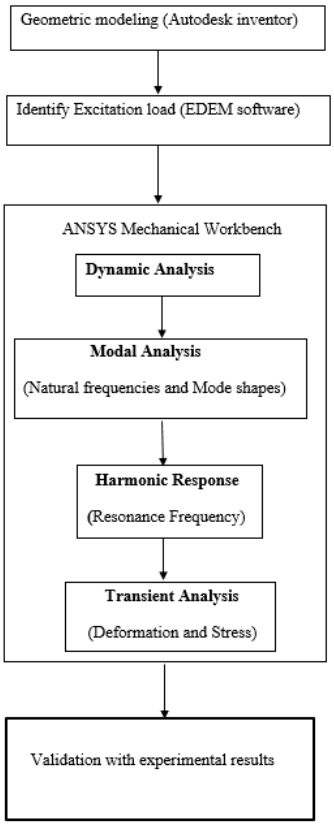

Figure 3.1: Vibration analysis procedure

3.2 Modeling of the Ball Mill

3.2.1 Sizing the Ball Mill Drum

The capacity of the drum was selected based on a case study of ball mills used by artisanal and small scale gold miners in Migori. Most commonly used ball mills have capacity of 100 kgs of ore charge. The drum internal parts and effective volume of the drum, are shown in Figure 3.2 and Table 3.1 respectively.

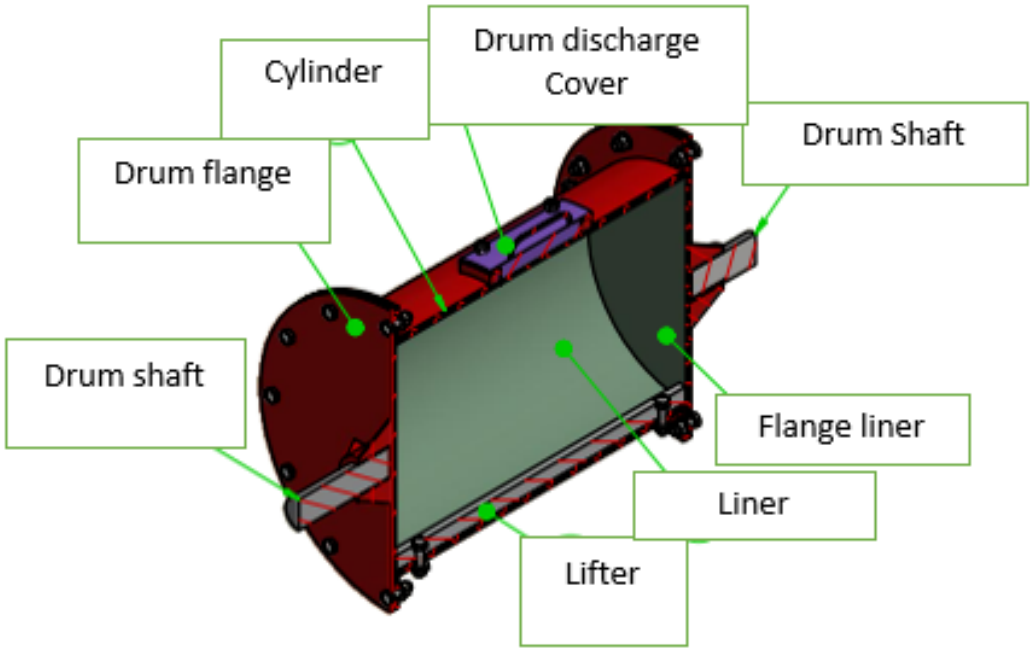

Figure 3.2: Drum parts

Table 3.1: Effective volume of drum

No	Part	Volume(mm^3)
1	Drum Internal	58690731
2	Drum cylinder liner	3113004
3	Side liners	1824668
4	Lifters	10451590
5	Effective Volume	52707900

Mass of grinding media, charge and drum were 94.24 kgs, 35.73 kgs and 68.28 kgs respectively. The total mass of the drum was 192.25 kgs.

3.2.2 Critical speed of the drum

The critical speed of the ball mill was calculated using equation 2.4.

Diameter of the drum is 362 mm, therefore, the critical speed of the ball mill (N) is 70.83 rpm. Ball mills operate at an optimum speed which is typically 70% of the critical speed (Toram, 2005). Thus, the mill speed is, 70% of N which is 49.48 rpm.

3.2.3 Geometric modeling of ball mill

A geometric representation of the ball mill developed in JKUAT is shown in Appendix II. A simplified model of the ball mill with essential part for analysis (Drum, Frame support and shaft) was modeled as shown in Figure 3.3.

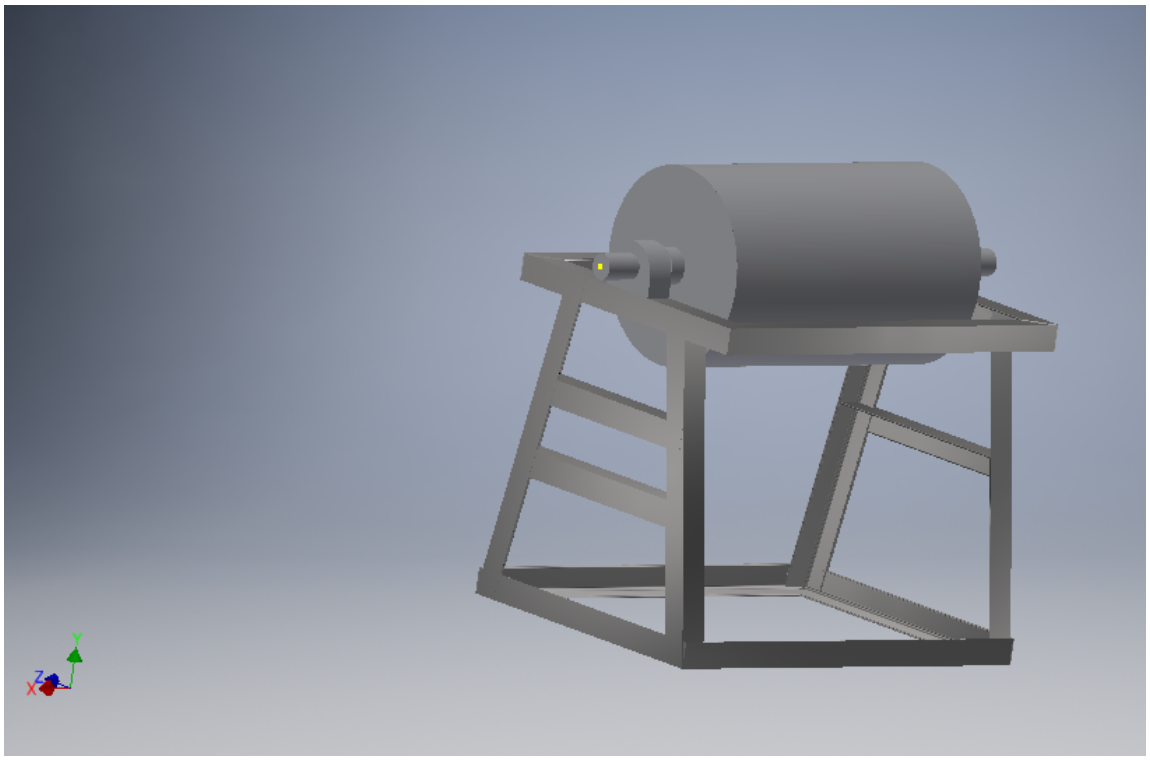

Figure 3.3: Simplified 3D model

The ball mill drum was also modeled in inventor and exported to EDEM software. In order to simplify the model and to reduce computational requirements such as time and memory, the size of the drum model was simplified. A ball mill can be represented by a slice, since length affects capacity of ball mill (Djordjevic, Shi, & Morrison, 2004; Powell, Weerasekara, Cole, LaRoche, & Favier, 2011; Jiang et al., 2018).

A 50 mm length slice DEM model of the mill was built then filled at 30% of the volume and then the number of balls was reduced which resulted in a reduction of simulation time. The 3D model of the slice of the drum is shown in Figure 3.4.

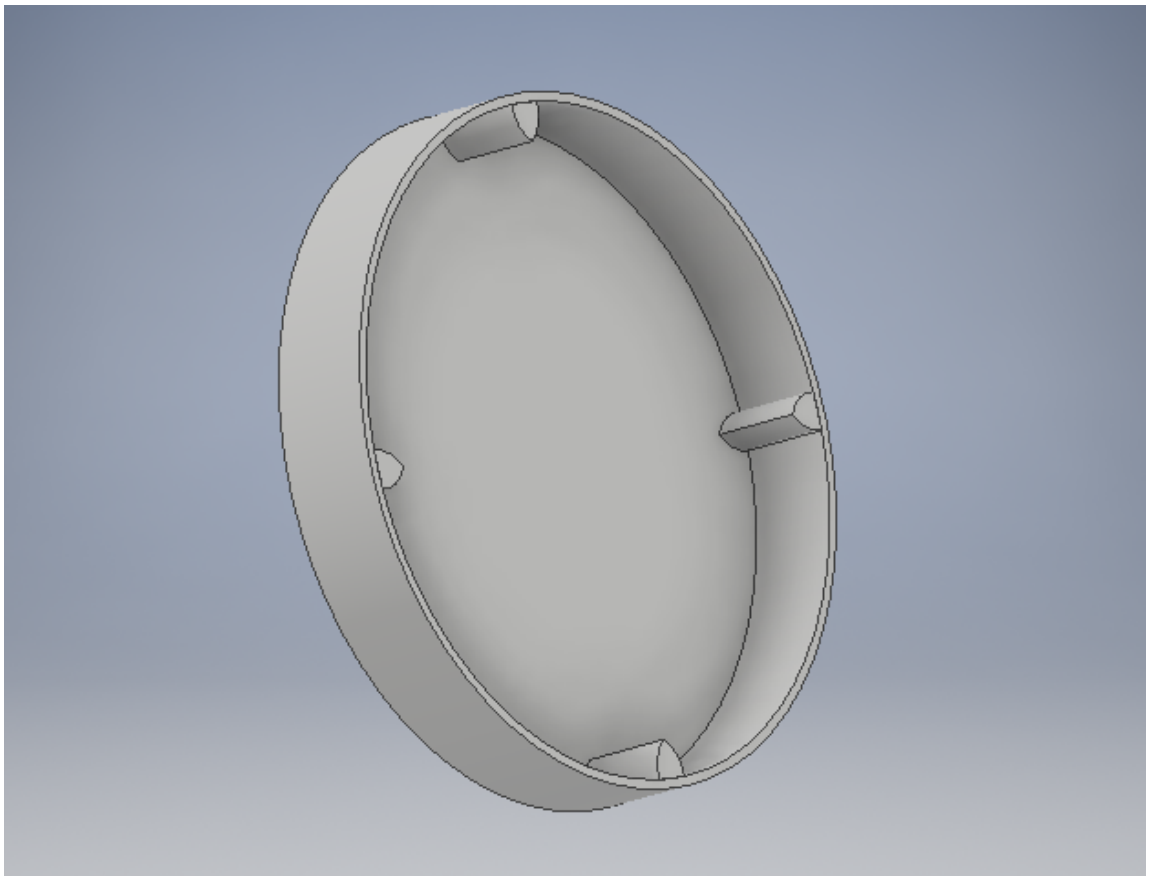

Figure 3.4: Model of slice of the full scale drum.

3.3 Discrete element analysis

The contact forces of charges inside the ball mill was obtained through DEM. In this research work discrete element method was carried out using EDEM software.

3.3.1 EDEM software

The setup used in EDEM software is shown in Figure 3.5

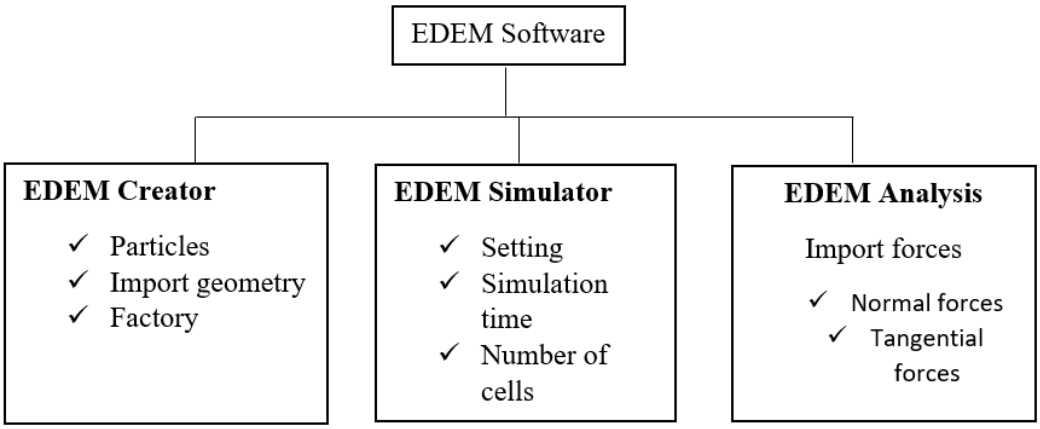

Figure 3.5: EDEM Set-up

Table 3.2: Simulation parameters

Poisson ratio	0.3
Density	$7850 kg/m^3$
Shear modulus	$7.5 \times 10^8 pa$
Operating speed	5.4467 rad/sec
Coefficient of restitution	0.5
Coefficient of static friction	0.74
Coefficient of rolling friction	0.002
Number of grinding balls	6000
Time step	2.3261×10^{-6}

The initial parameters to create a simulation in the EDEM software are shown in Table 3.2. The density, shear modulus, operating speed, number of grinding balls and time step were calculated, whereas the poison ratio, coefficient of restitution, coefficient of static friction and coefficient of rolling friction were adopted from the work of Kulya (Kulya, 2008). Boundary conditions where the time step of 2.3261×10^{-6} and the periodic boundaries of particle factory that were set in x,y and z directions.

Figure 3.6 shows the charges inside the drum during simulation.

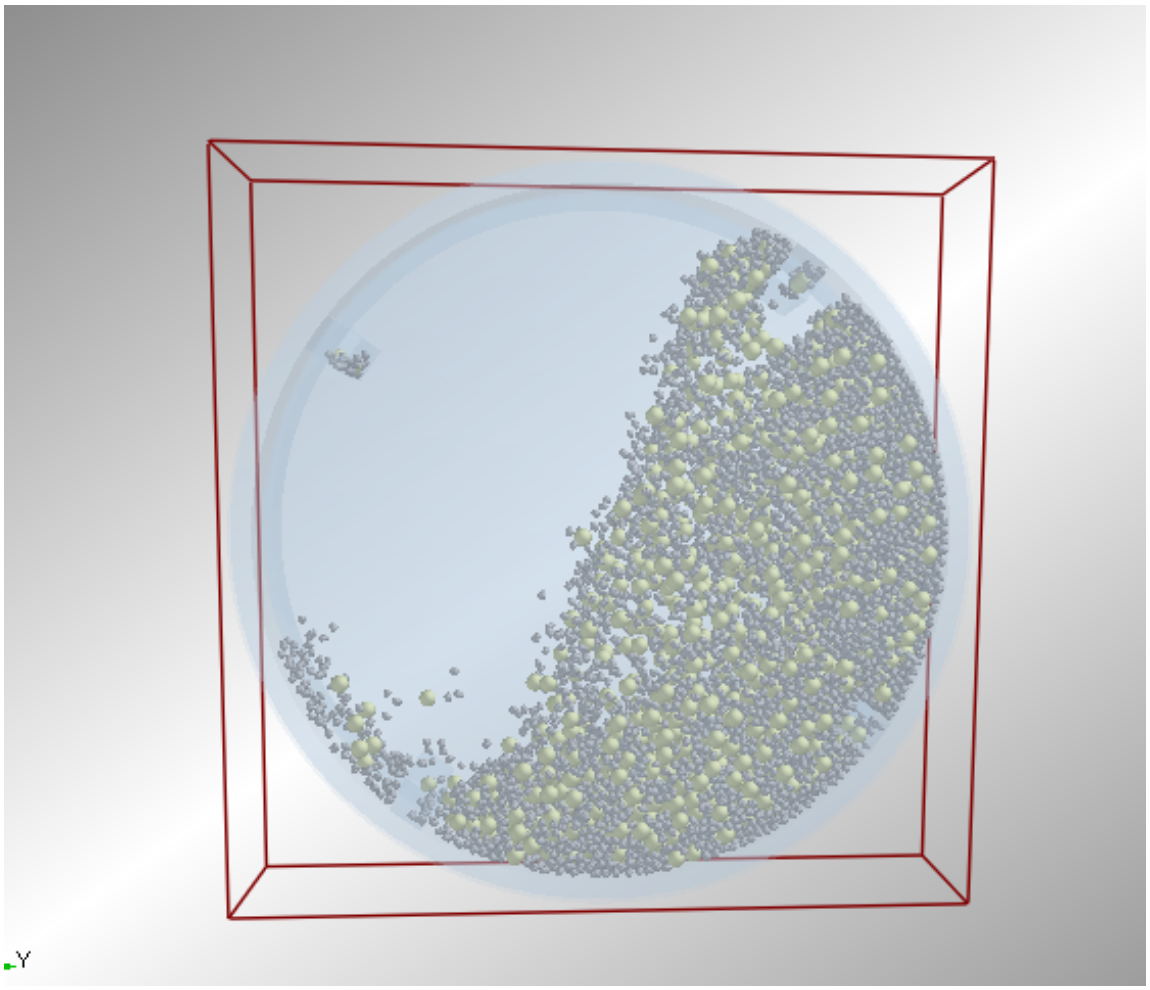

Figure 3.6: Charges inside the drum

3.4 Finite Element Modeling of the ball mill

ANSYS workbench 18.1 was used for the simulation. The dynamic characteristics were determined through three different analyses: modal, harmonic and transient analyses.

The dynamic equation of motion is shown in Equation 3.1.(Rao, 2010).

$$[m]\{\ddot{u}\} + [c]\{\dot{u}\} + [K]\{u\} = \{F(t)\}, \tag{3.1}$$

where $[m]$ is mass Matrix, $[c]$ is damping matrix, $[K]$ is stiffness matrix, $\{\dot{u}\}$ is nodal velocity, $\{\ddot{u}\}$ is nodal acceleration, $\{u\}$ is nodal displacement and $\{F(t)\}$ is the excitation

Force. The steps used in ANSYS workbench for finite element analysis process are shown in Figure 3.7.

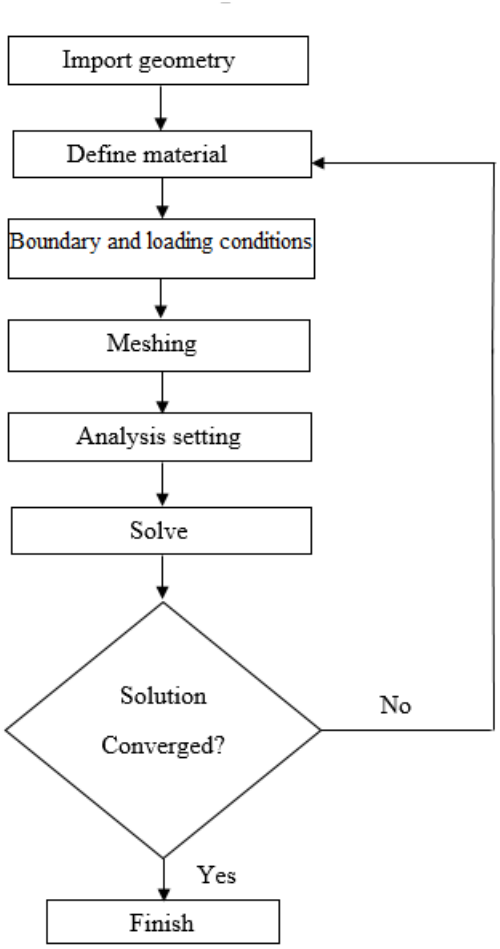

Figure 3.7: Flow chart of FEA process

3.4.1 Geometry Setup

The simplified three-dimensional ball mill was imported into ANSYS 18.1 workbench, by using STandard for the Exchange of Product data (STP) file extension.

3.4.1.1 Defining material

Material considered for ball mill structure was the structural steel. Since structural steel exhibits desirable physical properties, it makes it the the most versatile structure material to use. Properties of structural steel used in this research are indicated in Table 3.3. The volume of the drum was $52,707,900mm^3$. The frame used was the angle bar type with size $L50 \times 50 \times 5$, this was chosen according to the first model developed.

Table 3.3: Properties of structural steel (Harvey & for Metals, 1982)

Properties	Value
Density (kgm^{-3})	7850
Young's Modulus (MPa)	2×10^5
Poission's Ratio	0.3
Yield Strength (MPa)	250
Shear Modulus (GPa)	29.6
Tensile Strength (MPa)	460

3.4.1.2 Boundary conditions

Figure 3.8 shows boundary conditions applied. A fixed support was applied at the bottom surface of the support base, and a revolute joint was used as a joint connection between the drum shaft and the frame support.

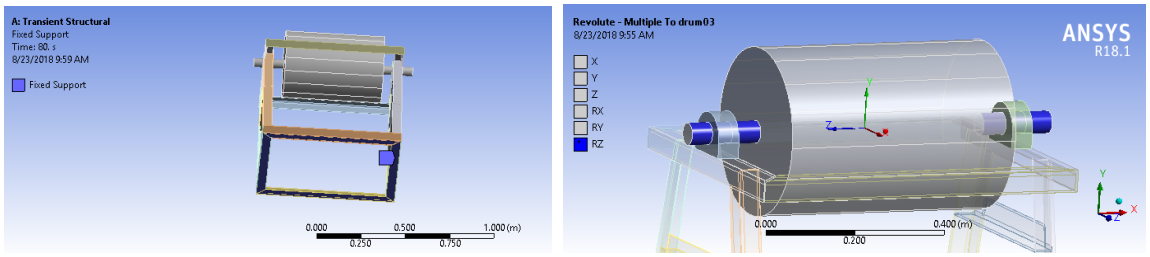

(a) Fixed Support (b) Revolute joint

Figure 3.8: Boundary conditions

3.4.1.3 Mesh generation

The ball mill model was meshed with hexahedral element since they are economic with the number of elements. The fine mesh are used with 175,853 nodes and 41,452 elements as it was the minimum number of element required for calculating acceptable results. A

fixed support was assigned to the lower surface of the support. The meshed geometry of ball mill is shown in Figure 3.9.

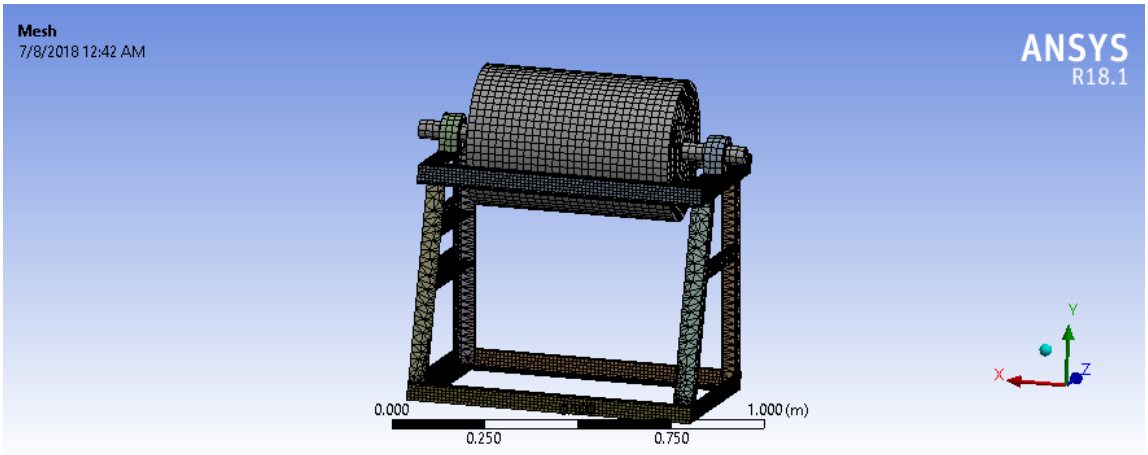

Figure 3.9: Meshed geometry of the ball mill

3.4.2 Modal analysis

Modal analysis was used to determine natural frequencies and mode shapes were used to investigate how the structure tended to vibrate at each frequency (He & Fu, 2001). Modal analysis was carried out before other dynamic analyses since it is the fundamental of other analyses ("ANSYS Mechanical, Modal Analysis", 2009). Damping is generally not taken into account, damping has virtually very little effect on its numerical results for natural frequencies (Joseph, William, & Allen, 1999) and that is why the eigenvalue problem was solved with undamped modal analysis and without considering excitation force. Therefore Equation 3.1 becomes;

$$[m]\{\ddot{u}\} + [K]\{u\} = \{0\}. \tag{3.2}$$

The free vibration mode of the structure is harmonic vibration, so the displacement is a sine function.

$$X = A\sin(\omega t). \tag{3.3}$$

Combining Equation 3.3 and 3.2 results:

$$([K] - \omega^2[M]) = 0. \tag{3.4}$$

Equation 3.4 represents an eigenvalue problem , where ω_i^2 are the eigenvalues and ω_i is the natural frequency.

The first 10 natural frequencies and vibration modes of the ball mill were extracted since lower order modes have a huge impact on vibration (Hao et al., 2016). Block Lanczos method was used to extract natural frequencies of the ball mill because it is a very efficient algorithm, (Yang, Yu, Zhang, & Cheng, 2017). The settings used in ANSYS are shown in Table 3.4.

Table 3.4: ANSYS settings

Object name	**Modal (A5)**
State	Solved
Physics Type	Structure
Analysis Type	Modal
Solver Target	Mechanical APDL
Environment Temperature	22^o C
Generate Input Only	No
Object Name	Pre-stress (None)
State	Fully Defined
Pre-Stress Environment	None

3.4.2.1 Convergence test for modal analysis

In order to achieve accurate results, mesh was refined. However, using over detailed mesh increases computation time (Olek Zienkiewicz, 2013). Several simulations were conducted and test was done on the first natural frequency as shown in Figure 3.10, in order to find an optimal mesh size.

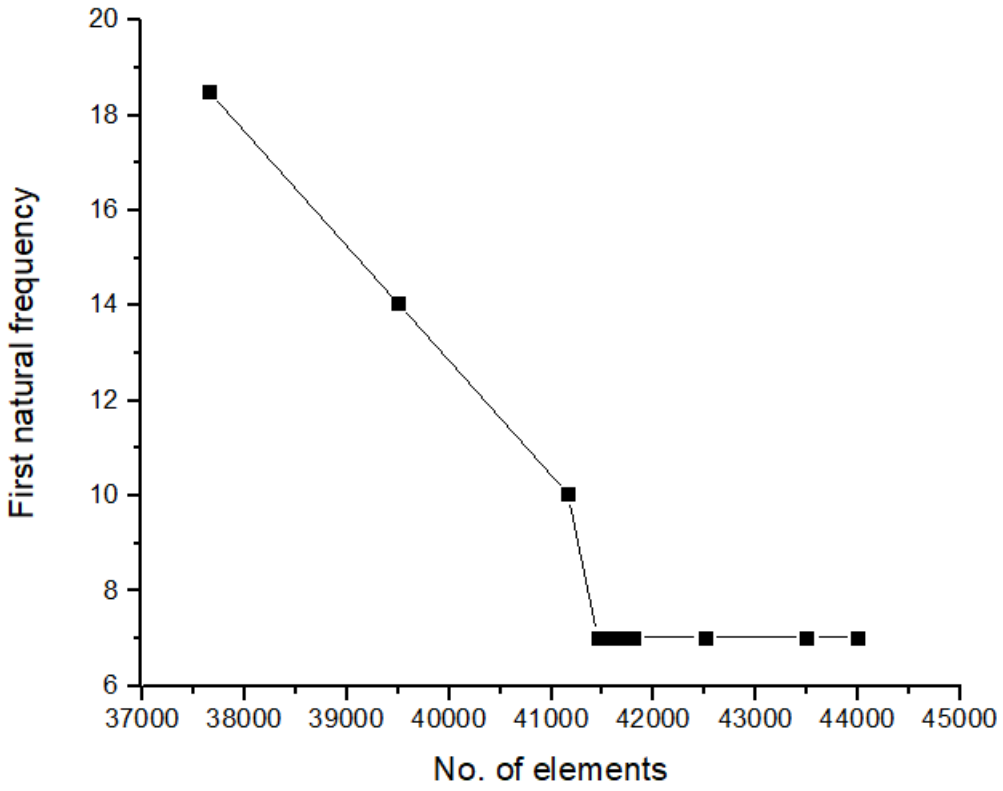

Figure 3.10: Convergence test for elements; first natural frequency

3.4.3 Harmonic Response

Harmonic response analysis was used to predict the sustained dynamic behaviour of the ball mill structure under predetermined excitation.

The frequency sweep range was set to 0-200 Hz since the operating frequencies of the ball mill vary in that range. The solution intervals were selected by considering the simulation time, and the solution method was set to the mode superposition since the modal analysis was already done.

The analysis settings used for harmonic response are shown in Table 3.5

Table 3.5: Analysis setting for harmonic response

State	Fully Defined
Range Minimum	0 Hz
Range Maximum	200 Hz
Solution Intervals	80
Solution Method	Mode Superposition
Cluster Results	No
Modal Frequency Range	Program Controlled

3.4.4 Transient analysis

Transient analysis was done to determine the time history dynamic response of the ball mill structure under the time-varying excitation forces. The equation of motion shown in Equation 3.1 was solved by ANSYS workbench mechanical, where $F(t)$ on the right hand side was taken to be the excitation forces from tumbling of media charge obtained from DEM simulation. The analysis yielded the displacement, velocity, acceleration, and stress time history response of the structure. The vibration amplitude, displacement, velocity and acceleration were used to indicate how good or bad the condition of the ball is by comparing with the standard limit.

To apply the excitation forces, the drum shell was subdivided into faces, since the charge media did not fill the whole ball mill drum and not all parts of the drum shell experienced the impact at the same time.

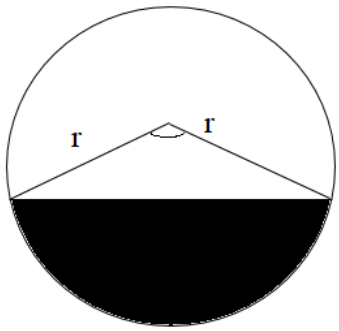

Figure 3.11: Ball mill filled at 30%

Face discretization was done as follows; considering the filling of 30% as this filling was used in experimental work, the area covered by the charge was calculated from Equation 3.5, and this area was subtended at the center of the ball mill by an angle of 142 ° as shown in Figure 3.11. Taking 360 dividing by 142 gives 2.54, and round off to 3. Therefore, the ball mill can be subdivided into three segments, and subsequently three faces, as shown in Figure 3.12. It was assumed one time step per face.

$$Area = \frac{\pi r^2}{[(\frac{\alpha}{360} \times \pi r^2) - (\frac{r^2}{2} \sin \alpha)]} = 10/3, \tag{3.5}$$

where, r is the radius of the drum which is 372 mm.

In order to apply the excitation forces, the drum was divided into three faces in direction parallel to the shaft as shown in Figure 3.12. At time t = 0s, no forces applied on faces, at time t= 1s, force is applied on face one, while on other faces no forces applied on them. At time t = 2 s, force is applied on face 2 and zero forces on other faces. The process continues up t=16 s as shown in Table 3.6 and 3.7.

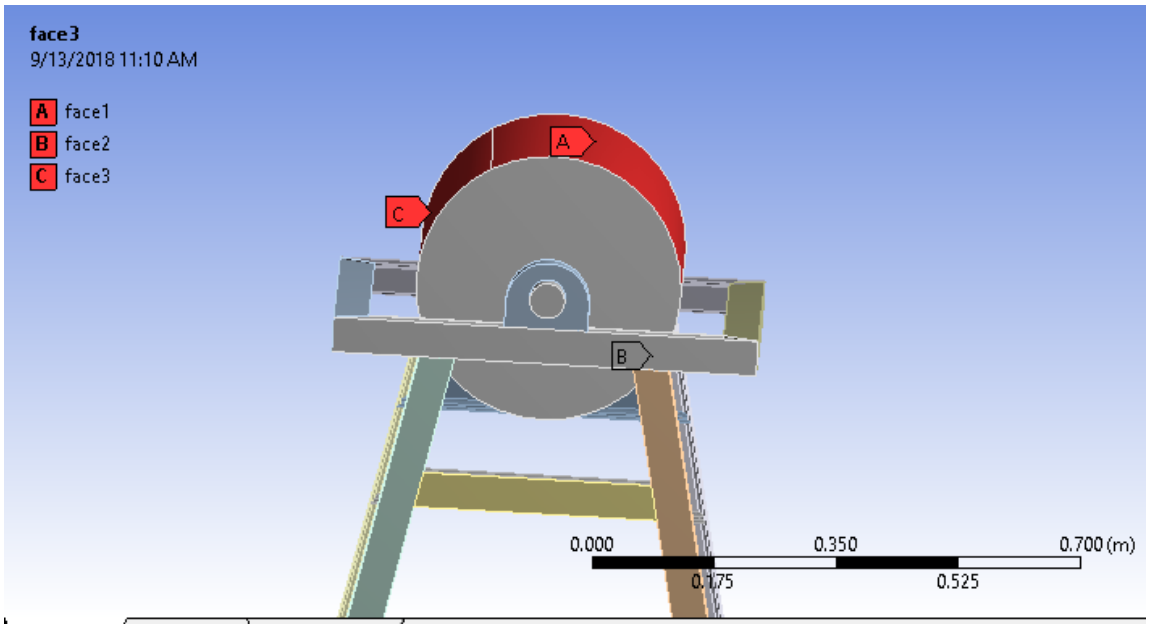

Figure 3.12: Faces used to apply load on the drum.

Table 3.6 and 3.7 illustrate how excitation forces were applied on the drum. These excitation forces were inserted to ANSYS using tabular data option.

Table 3.6: Application of excitation forces on the drum (A)

Time (s)	Face 1		face 2		Face 3		face 1		Face 2		Face 3		Face 1		Face 2	
	F_n (N)	F_t (N)	F_n (N)	F_t (N)	F_n (N)	F_t (N)	F_n (N)	F_t (N)	F_n (N)	F_t (N)	F_n (N)	F_t (N)	F_n (N)	F_t (N)	F_n (N)	F_t (N)
0	0	0	0	0	0	0	0	0	0	0	0	0	0	0	0	0
1	-912.5	264.56	0	0	0	0	0	0	0	0	0	0	0	0	0	0
2	0	0	-248.44	94.76	0	0	0	0	0	0	0	0	0	0	0	0
3	0	0	0	0	-1191.32	248.87	0	0	0	0	0	0	0	0	0	0
4	0	0	0	0	0	0	-436.8	285.86	0	0	0	0	0	0	0	0
5	0	0	0	0	0	0	0	0	-1869.89	636.63	0	0	0	0	0	0
6	0	0	0	0	0	0	0	0	0	0	-822.12	274.4	0	0	0	0
7	0	0	0	0	0	0	0	0	0	0	0	0	-859.4	398.54	0	0
8	0	0	0	0	0	0	0	0	0	0	0	0	0	0	-615.05	251.5

Table 3.7: Application of excitation forces on the drum (B)

Time (s)	Face 3		face 1		Face 2		face 3		Face 1		Face 2		Face 3		Face 1	
	F_n (N)	F_t (N)	F_n (N)	F_t (N)	F_n (N)	F_t (N)	F_n (N)	F_t (N)	F_n (N)	F_t (N)	F_n (N)	F_t (N)	F_n (N)	F_t (N)	F_n (N)	F_t (N)
0	0	0	0	0	0	0	0	0	0	0	0	0	0	0	0	0
9	-1068	476.1	0	0	0	0	0	0	0	0	0	0	0	0	0	0
10	0	0	-741.8	331.6	0	0	0	0	0	0	0	0	0	0	0	0
11	0	0	0	0	-1192.8	379.5	0	0	0	0	0	0	0	0	0	0
12	0	0	0	0	0	0	-721	294.34	0	0	0	0	0	0	0	0
13	0	0	0	0	0	0	0	0	-970.922	497.5	0	0	0	0	0	0
14	0	0	0	0	0	0	0	0	0	0	-688.13	302.87	0	0	0	0
15	0	0	0	0	0	0	0	0	0	0	0	0	-1251.8	464.8	0	0
16	0	0	0	0	0	0	0	0	0	0	0	0	0	0	-782.95	234.7

3.4.4.1 Analysis Settings

The time step used in transient analysis was calculated from natural frequency results using Equation 3.6 (Morgan, 2015).

$$\Delta t_{initial} = \frac{1}{20 f_{reponse}} \tag{3.6}$$

where $f_{response}$ is the frequency of the highest mode of interest. The corresponding frequency of the tenth mode is 204.39Hz. Therefore, the initial time step was 0.00025 which was used as the minimum time step. The upper bounds of the time step was set to 0.005 to prevent indefinite solutions. Figure 3.13 shows the settings used in ANSYS.

Details of "Analysis Settings"	
Step Controls	
Number Of Steps	1.
Current Step Number	1.
Step End Time	80. s
Auto Time Stepping	On
Define By	Time
Initial Time Step	2.5e-004 s
Minimum Time Step	2.5e-004 s
Maximum Time Step	0.3 s
Time Integration	On
Solver Controls	
Solver Type	Program Controlled
Weak Springs	Off
Large Deflection	On
Restart Controls	
Generate Restart Po...	Program Controlled
Retain Files After Fu...	No
Combined Restart Fi	Program Controlled

Figure 3.13: Transient analysis settings

3.4.4.2 Convergence Criteria

The Newton-Raphson residuals were used to test the convergence of the simulation. If the force convergence value (residual force) is smaller than that of force criterion the step is said to have converged. If not another iteration takes place. The iteration continues until the convergence criterion is satisfied (Lee, 2018; ANSYS, 2017). Force and displacement convergence are shown in Figure 3.14 and 3.15 Respectively. The last cumulative iteration from the solver output is shown in Appendix III.

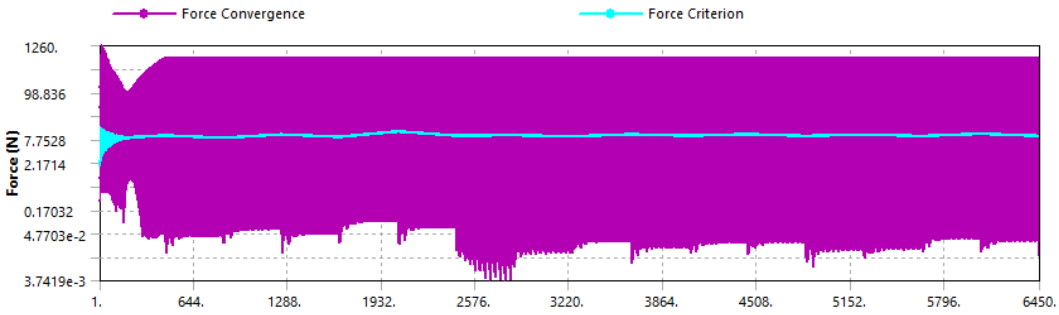

Figure 3.14: Force convergence

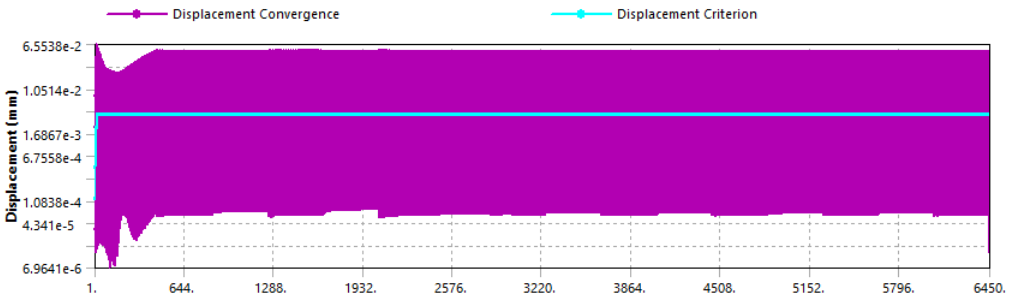

Figure 3.15: Displacement convergence

3.5 Experimental Work

In this section, method used in experimental work carried out on the ball mill are discussed. The experiment was conducted at the workshop in JKUAT. The purpose of the experiment was to analyze the vibration of the ball mill structure in order to validate the numerical results.

3.5.1 Experimental setup

Figure 3.16 and 3.17 show the schematic and pictorial views of experimental setup.

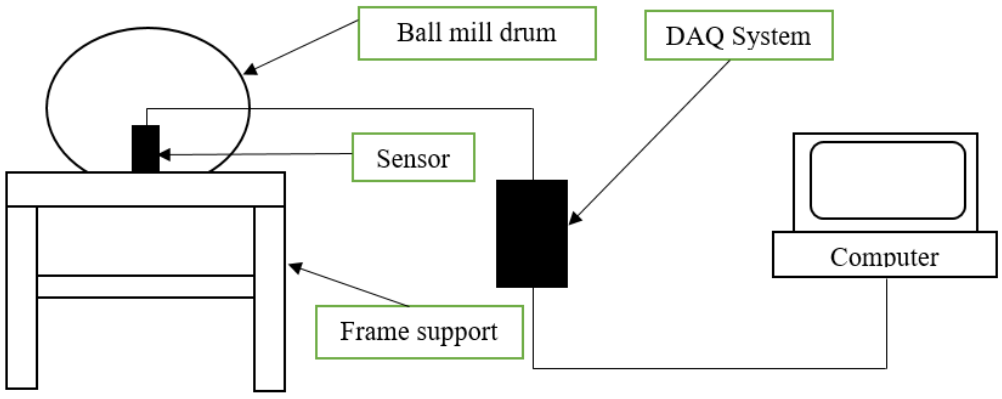

Figure 3.16: Schematic view of the experimental setup

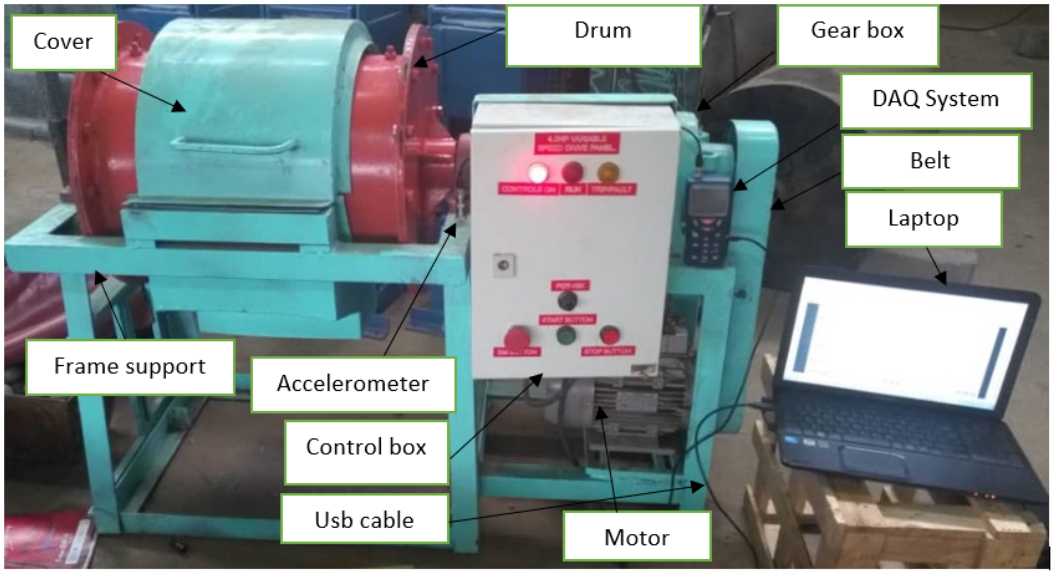

Figure 3.17: Pictorial view of the experimental setup

3.5.2 Data acquisition setup

The data acquisition setup helps to collect real physical quantities such as, acceleration, velocity and displacement, and convert them into digital signals, which are interpreted and processed by computers. Data acquisition setup comprised of a sensor to collect the physical data and convert them to electrical signals. These electrical signals are interpreted by the computers through data acquisition hardware.

3.5.2.1 Accelerometer

Accelerometers are sensors commonly used for vibration measurement. They are used to measure the dynamic acceleration of the physical device. In this experiment, they were used to sense acceleration, displacement and velocity of the structure of the ball mill. The piezoelectric accelerometer PA-01 was used to measure the vibrations that was then convert into electrical signals using piezoelectric effect. Piezoelectric type accelerometers have a built-in amplifiers, hence they do not require external amplifiers. The amplified electrical signals from the accelerometer are sent to DAQ hardware through a curled cable (VA-02). Figure 3.18 shows the accelerometer.

Figure 3.18: PA-01 Piezoelectric accelerometer

The accelerometer has a very powerful magnetic attachment (0.8kG-1.0kG), which helped in mounting it on the structure of the ball mill.

3.5.2.2 Data Acquisition Hardware

The analogue signal received from the amplifier is converted to digital signal by the DAQ hardware using analog to digital convertor. The DAQ hardware is the interface between the signal acquired from the sensor and the computer. After getting the digital signal, it is then sent to the computer for data analysis and storage. The DAQ hardware used is the TES-3101 vibration meter model. The digital signal from the DAQ hardware is sent to the computer through USB cable.

3.5.3 Test method

The ball mill was filled by steel balls and materials by 30% of filling as shown in Figure 3.19, and then the ball mill was tested in dry condition and at different rotation speeds (50-100% of critical speed), by using a tachometer. For each experimental condition, the ball mill was allowed to run for a few seconds so that the rotation speed reach a stable status. Table 3.8 shows the experimental conditions.

Table 3.8: Conditions of the experiment

Mill	Diameter	372 mm
	Length	540 mm
	Speed (rpm)	35, 42, 49, 56, 63 and70 rpm
	% of critical speed	50, 60, 70, 80, 90, 100
	Filling	30 % of the total volume
Lifters	Number	4
	Shape	Rectangular
Grinding media	Material	Steel balls
	Ball diameter	1 mm
Feed	Material	Basalite

Figure 3.19: Drum with 30% filling

Tests were carried out at two locations (A,B) as shown in Figure 3.20, where amplitude of vibration in terms of acceleration were measured. These two locations were considered to be subjected to high vibration amplitude, since it is where the drum contact the frame support.

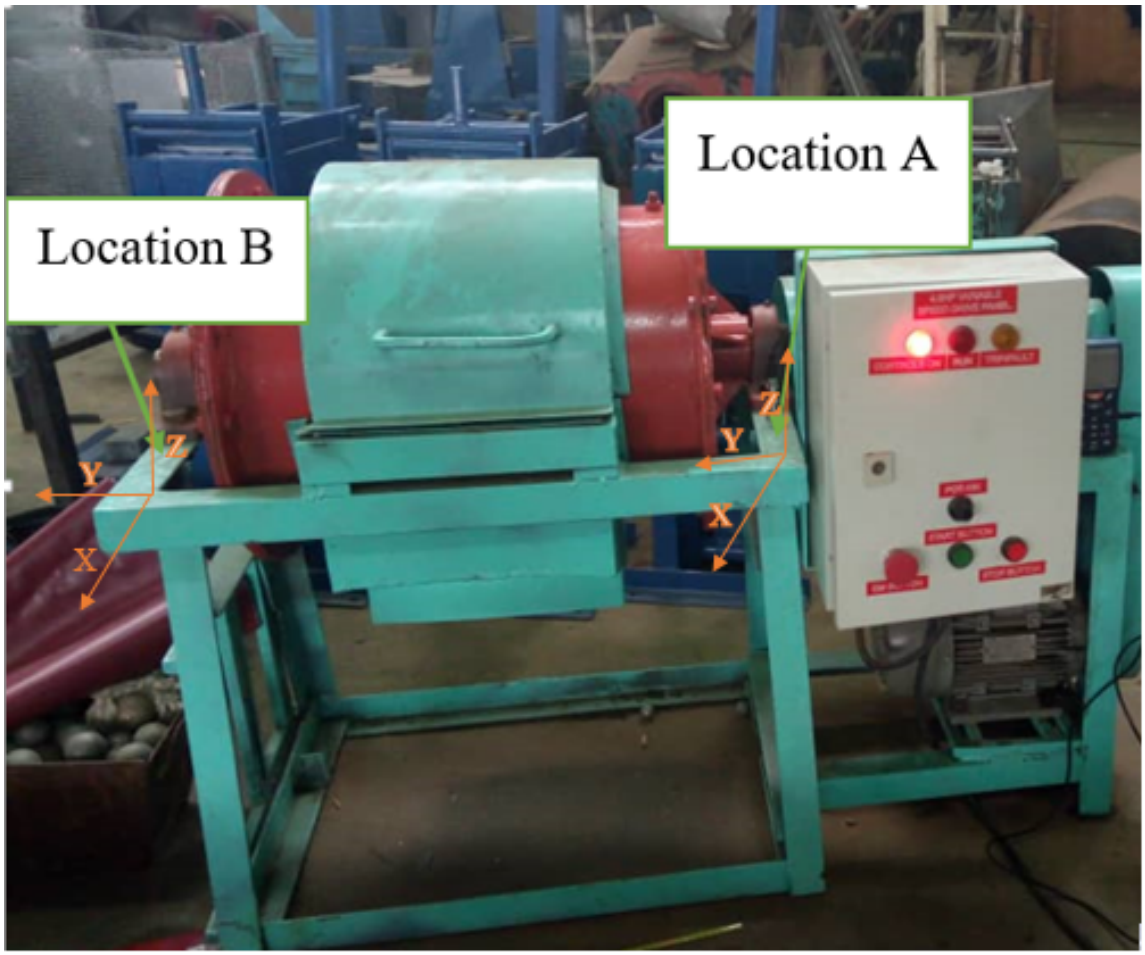

Figure 3.20: Location of the measured points

3.6 Model validation

To check whether the simulation results reflect the physical behaviors of the ball mill. The simulation results obtained were validated by comparing with the results obtained from experimental work. Figure 3.21 shows a comparison between the simulation and the experimental results.

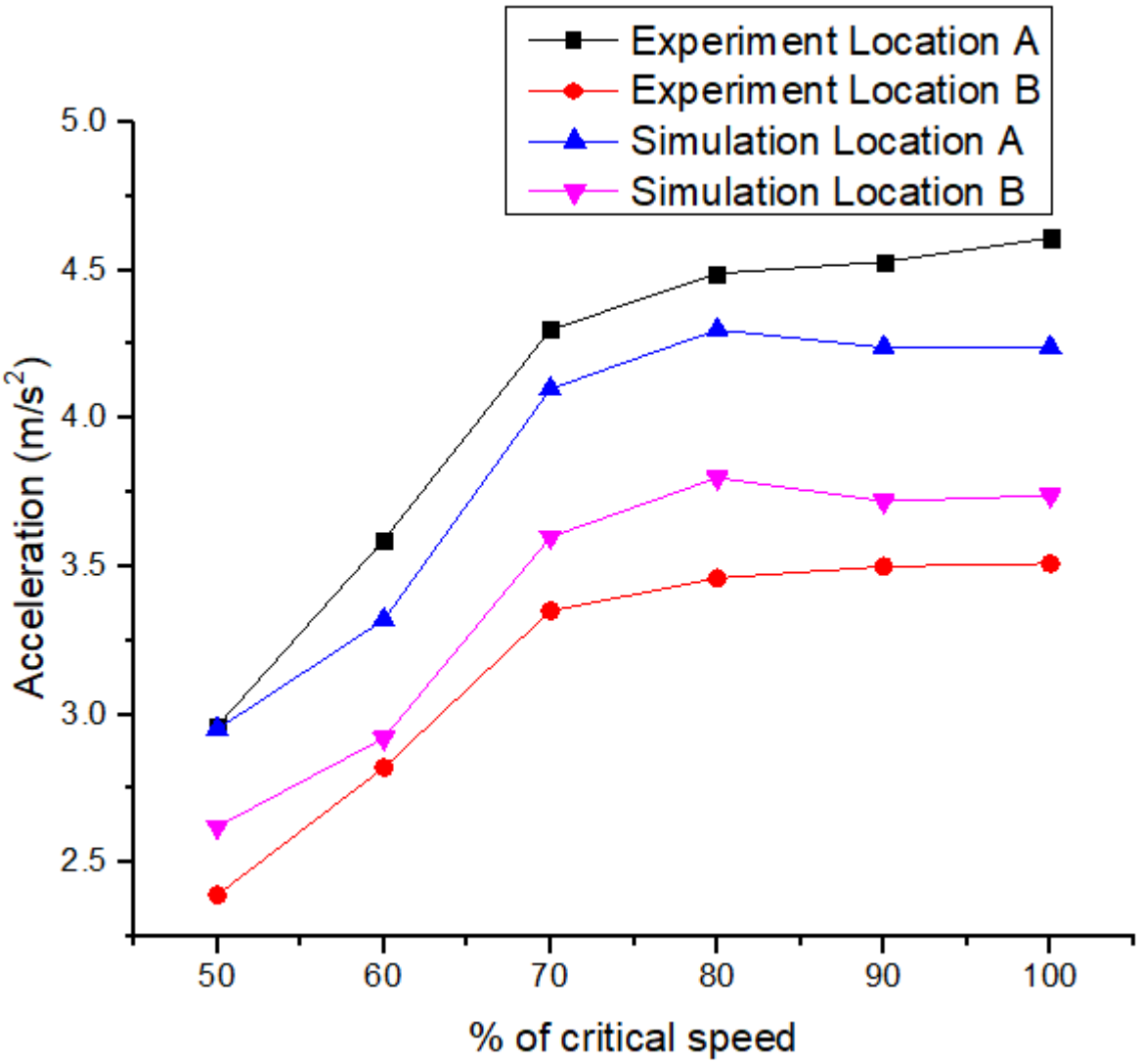

Figure 3.21: Simulation and experimental results

It is seen that for both simulation and experiment vibration amplitude increase as the rotation speed increase until 80% of critical speed, where the vibration amplitude start reducing.

Table 3.9: Deviations between simulation and experiment

Critical speed	**Location A**		**Location B**		**Deviation (%)**	
%	Experiment	Simulation	Experiment	Simulation	A	B
50	2.96	2.95	2.39	2.62	0.34	8.7
60	3.59	3.32	2.82	2.92	7.5	3.4
70	4.3	4.1	3.35	3.6	4.6	6.9
80	4.49	4.3	3.46	3.8	4.2	8.9
90	4.53	4.24	3.5	3.72	6.4	5.9
100	4.61	4.24	3.51	3.74	8	6.2

Table 3.9 shows the variation between measured and simulated values. The mean error is 5.9 %, this can be attributed to assumptions made during FEM simulation in simplification of the model. For example the motor and belt were not included in the developed model. Uncertainties of normal and tangential stiffness during DEM analysis (Jonsén, Stener, I.Palsson, & Hans-Ake, 2013) can also be the source of these variation. Also discrepancies might be caused by external noise.

CHAPTER FOUR
RESULTS AND DISCUSSION

4.1 Introduction

This chapter presents the results of DEM and FEM (modal, harmonic response and transient analysis) that were done through simulation. The results of experimental work, are also presented here.

4.2 Contact forces

Contact forces were calculated in EDEM simulation. The forces obtained were for a small slice of the drum; hence forces were integrated to the full length of the drum. The impact forces obtained were used as excitation forces for the dynamic analysis of the ball mill structure. Several simulations were conducted and the trend was confirmed to be random time-varying as shown in Figure 4.1.

The maximum normal and tangential forces were 1869.9 N and 636.635N respectively and occurred within the first second. At time $t = 0sec$, impact forces were zero because the ball mill was at rest. Forces became higher at 1 second because the rotation velocity of the ball mill was fluctuating. The rotation speed of the ball mill stabilized after 1 second and this was proven in experimental work by the use of a Tachometer.

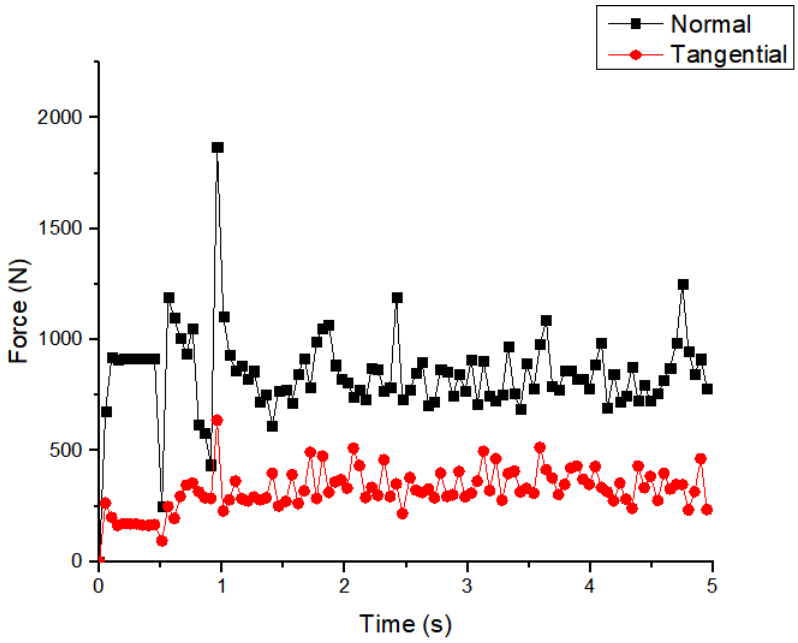

Figure 4.1: Impact forces

Impact forces depend on many factors: the mill filling, the rotation speed of the drum, the lifter number and the grinding time.

When the mill filling is increased, the impact forces decrease. At high volume of mill, the height of the fly becomes less. At low volume,the charge particles come down rapidly which results in high impact forces. However, higher impact can lead to fracture and wear of the liner. From Figure 4.1, peak impact forces were observed when charges reached a lifter. This can be explained from Equation 2.10 and 2.14 for normal and tangential forces respectively. As the charge is lifted to the top, it falls to the wall of drum from a maximum height with maximum velocity resulting in high impact forces. However, as the time goes on, particles are ground and impact forces become less. An FFT of the contact forces was carried out as shown in Figure 4.2 and 4.3 in order to obtain the dominant frequency.

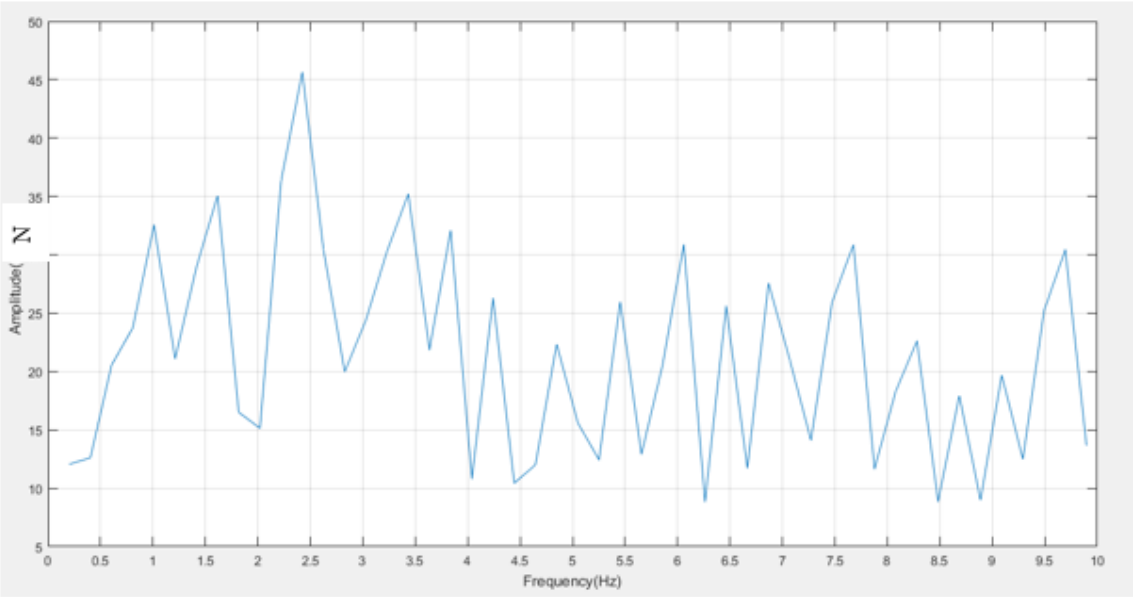

Figure 4.2: Normal forces frequency domain

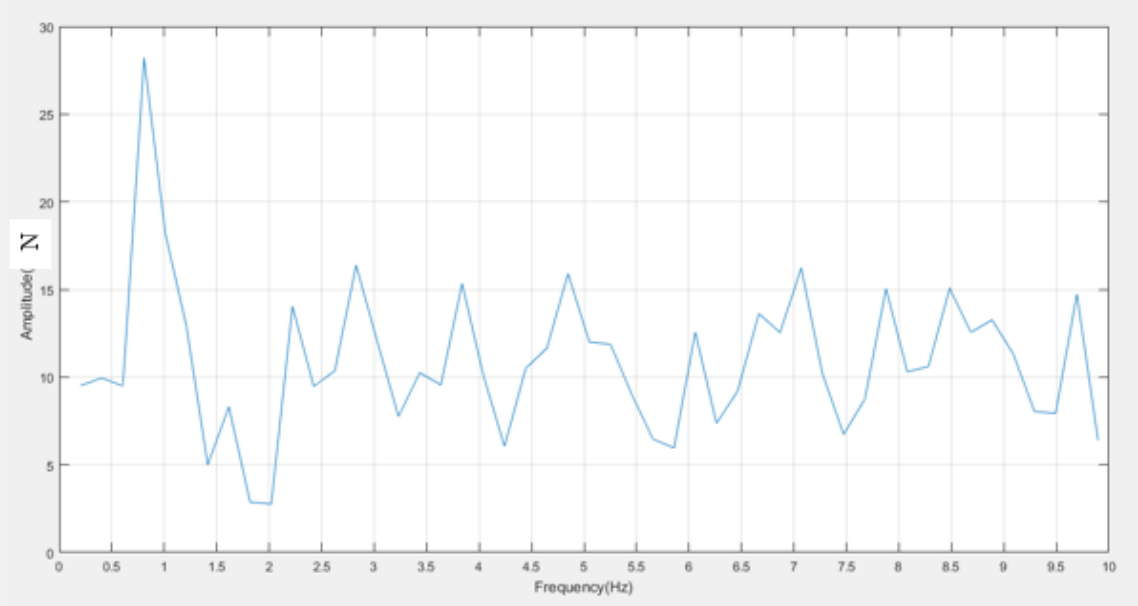

Figure 4.3: Tangential forces frequency domain

The frequencies with the highest peak amplitude were 2.4 Hz and 0.8 Hz for normal and tangential contact forces respectively.

4.3 Modal Analysis

Modal analysis was used to obtain the first ten natural frequencies and their corresponding mode shapes for the ball mill structure since the lower natural frequencies have huge impact on the vibration. After carrying out several simulations, it was found out that at 41452 elements the first natural frequency started to converge. It was therefore assumed that 41452 elements was the minimum number of elements required for calculating acceptable results.

The first 10 natural frequencies and corresponding mode shapes of the ball mill structure are presented in this section.

4.3.1 Natural frequencies

The first ten natural frequencies of ball mill structure were as shown in Table 4.1. The natural frequencies obtained were in the between 0-205 Hz.

Table 4.1: Frequencies and corresponding vibration modes

Mode	Frequency (Hz)	Type of mode
1	7.02	Bending along X axis
2	26.6	Bending along Z axis
3	47.6	Bending along ZX axis
4	59	Twisting along Y axis
5	65.4	Twisting along Y axis
6	133.3	Twisting along X axis
7	154.5	Bending along Z axis
8	157.4	Bending along Z axis
9	198.4	Bending along Z axis
10	204.4	Bending along Z axis

The bar chart shown in Figure 4.4 indicates frequency at each calculated mode. The X-axis contains number of modes and the Y-axis contain frequencies.

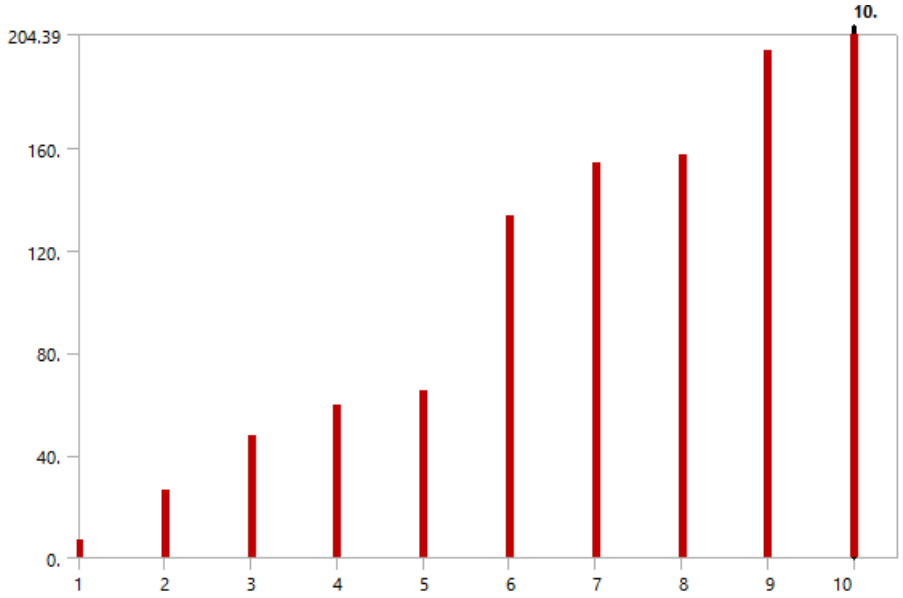

Figure 4.4: Frequency vs variation of number of modes.

4.3.2 Mode shapes

The ten modal shapes corresponding to the calculated natural frequencies were as shown in Figure 4.5.

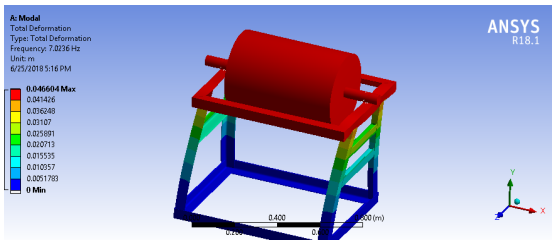

(a) The 1st mode

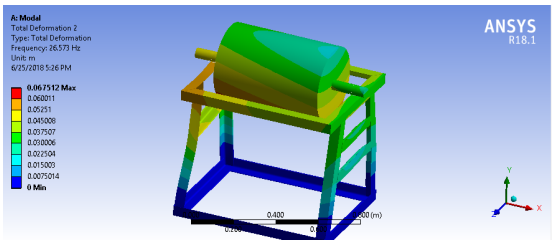

(b) The 2nd mode

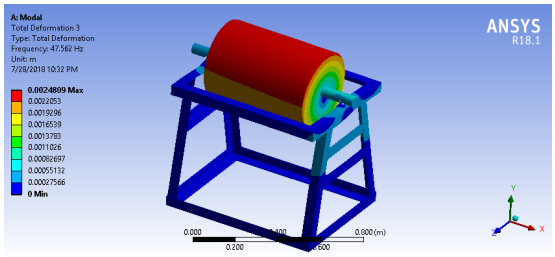

(c) The 3rd mode

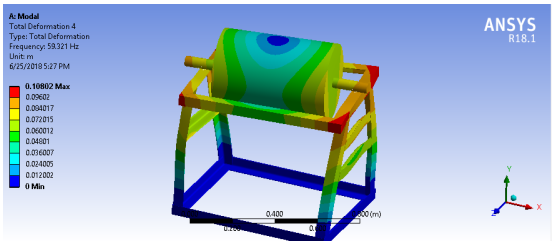

(d) the 4th mode

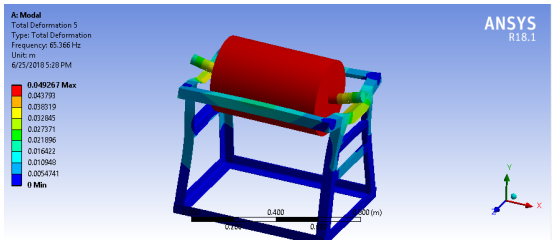

(e) the 5th mode

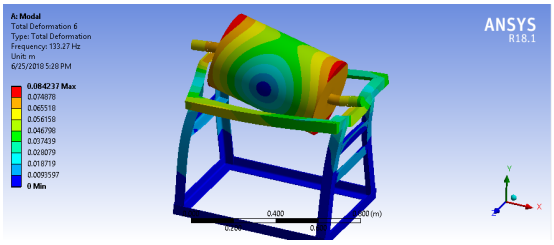

(f) the 6th mode

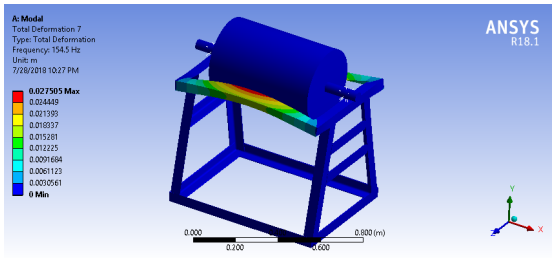

(g) the 7th mode

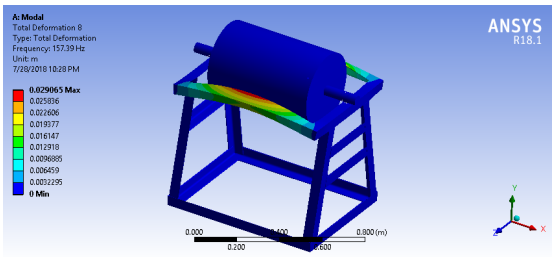

(h) the 8th mode

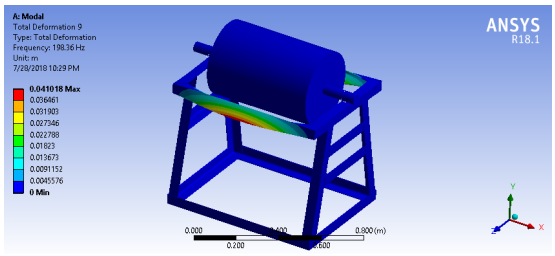

(i) the 9th mode

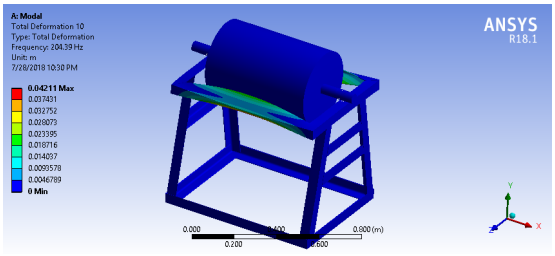

(j) the 10th mode

Figure 4.5: Mode shapes of ball mill structure

The vibration mode of the first order natural frequency was bending along the X-axis with the highest deformation located on the drum as shown in Figure 4.5a. The vibration mode of the second order natural frequency was found to be bending along the Z-axis with the highest deformation located on the frame as shown in Figure 4.5b. The vibration mode for the third order natural frequency was bending along the Z-axis with the highest deformation being on the frame support as shown in Figure 4.5c. The fourth and fifth order natural frequencies were close but had different modes of vibration. The vibration of the fourth order natural frequency was twisting along Y axis with the maximum deformation being on the drum as shown in Figure 4.5d). The vibration mode of the fifth order natural frequency was bending along Y axis with the maximum vibration being on the ball mill as shown in Figure 4.5e. The mode of vibration of the sixth order natural frequency was twisting along Y axis with highest deformation being on the drum and on the frame support as shown in Figure 4.5f. The mode of vibration obtained for the seventh ,eighth, ninth and tenth order natural frequencies were bending along Z axis with the maximum vibration on the top part of the frame support as shown in Figure 4.5g, 4.5h, 4.5i ,and 4.5j respectively.

The first natural frequency obtained was 7 Hz. The frequencies from operating speed of ball mill varied from 0 to 1.67 Hz depending on the rotation speed and the dominant

frequency from the tumbling of charge was 2.4 Hz. Therefore, the first natural frequency was higher than the operating frequency of the ball mill. This showed that the natural frequencies were outside the limits of the operating frequency of the ball mill structure. To avoid resonance, the first natural frequency should have been less than $0.7f$ or larger than $1.4f$ where f is the operating frequency of the machine (Han & Guevara, 2013). Therefore, there was no risk of resonance in the ball mill structure. However, for the fifth and sixth order vibration modes, as shown in Figure (4.5e and 4.5f respectively, it was obvious that the whirling of the shaft caused by loading of the drum introduced some vibration which could have a high amplitude.

4.3.3 Modal analysis results for drum and shaft

Damped frequency (Hz), stability (HZ), modal damping ratio and logarithmic decrement obtained were as illustrated in Figure 4.6.

Set	Solve Point	Mode	Damped Frequency [Hz]	Stability [Hz]	Modal Damping Ratio	Logarithmic Decrement
1.	1.	1.	9.834e-004	3.2577e-011	-3.3127e-008	2.0814e-007
2.		2.	6.2216e-003	-2.773e-009	4.4571e-007	-2.8005e-006
3.		3.	20.247	-0.37175	1.8358e-002	-0.11537
4.		4.	20.34	-0.37701	1.8532e-002	-0.11646
5.		5.	86.108	-6.9027	7.9907e-002	-0.50368
6.		6.	86.451	-6.6066	7.6197e-002	-0.48016
7.		7.	0.	-200.14	1.	N/A
8.		8.		-204.07		
9.		9.	302.63	-29.084	9.5663e-002	-0.60384
10.		10.	306.49	-29.822	9.6844e-002	-0.61136
11.	2.	1.	9.834e-004	3.1092e-010	-3.1617e-007	1.9865e-006
12.		2.	6.2216e-003	-2.7317e-009	4.3906e-007	-2.7587e-006
13.		3.	20.246	-0.37169	1.8356e-002	-0.11535
14.		4.	20.341	-0.37707	1.8534e-002	-0.11648
15.		5.	74.044	-5.7744	7.775e-002	-0.49
16.		6.	100.54	-7.704	7.6405e-002	-0.48147
17.		7.	0.	-200.21	1.	N/A
18.		8.		-204.06		
19.		9.	302.63	-29.084	9.5663e-002	-0.60384
20.		10.	306.49	-29.822	9.6844e-002	-0.61137

Figure 4.6: Damped frequency (Hz), stability (Hz), modal damping ratio and logarithmic decrement.

Figure 4.7 shows the frequency at each calculated mode

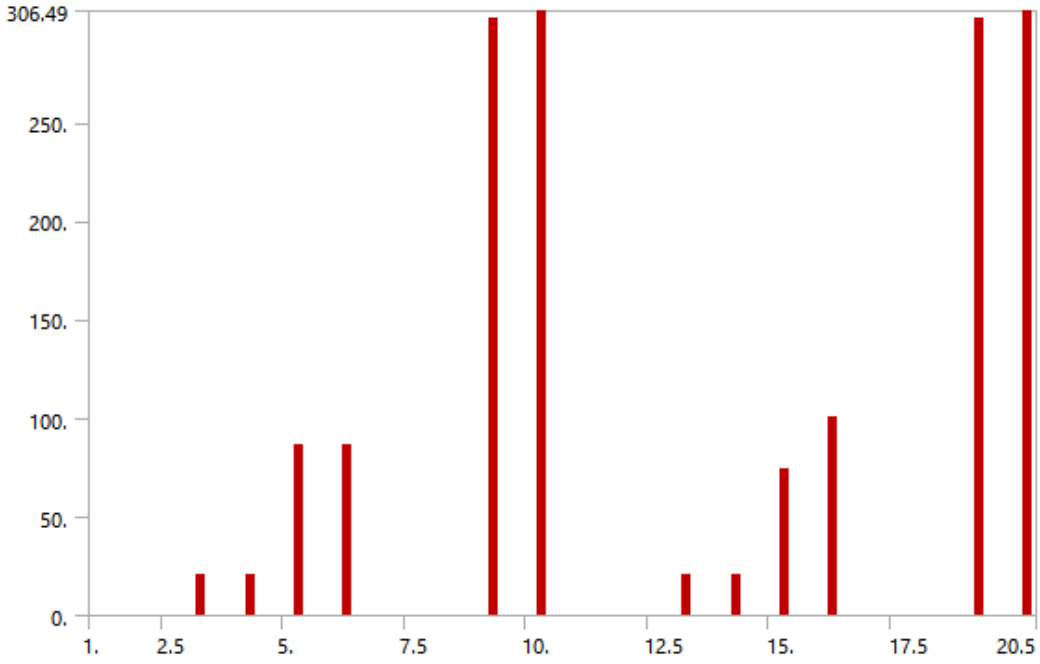

Figure 4.7: Frequency at each calculated mode

4.3.3.1 Mode shapes

Out of the first ten order modes extracted using Block Lanczos method, four of them were as illustrated in Figure 4.8.

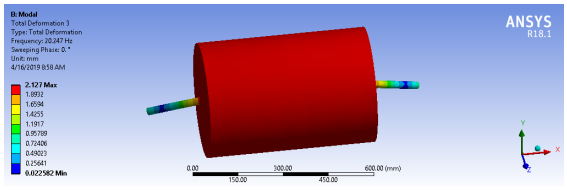

(a) the 3rd mode

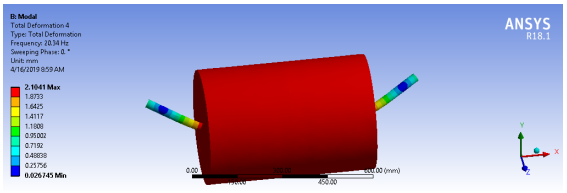

(b) the 4th mode

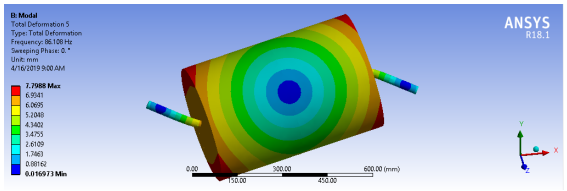

(c) the 5th mode

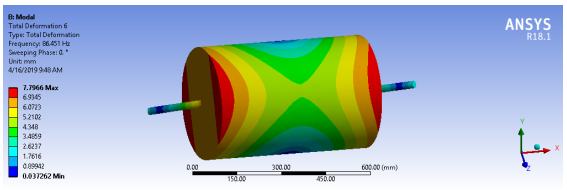

(d) the 6th mode

Figure 4.8: Mode shapes of ball mill drum.

The 4th and 5th mode shown in Figure 4.8b and 4.8c respectively revealed that the shaft deflections were high, hence the vibrations had high amplitude. Consequently, the stiffness of the shaft needs to be enhanced.

From the modal analysis carried out on the two models (ball mill and and ball drum only), it was seen that the stiffness of structure was not enough in transverse direction as shown in Figure 4.5d and 4.5f. The stiffness of the shaft also needs to be increased as Figure 4.8b and 4.8c showed that it was not enough. The rotation speed of the ball mill also influenced the vibration as the whirling of the shaft depended on the rotation speed.

4.4 Harmonic Response

The frequency response of ball mill structure obtained from ANSYS was as shown in Figure 4.9. By using harmonic response it is easy to visualize which frequencies are creating the highest deformation and from this result it is easier to find the eigen mode of the ball mill structure. The force considered was 1869.9 N as this was the maximum amplitude of the forcing function obtained from EDEM analysis.

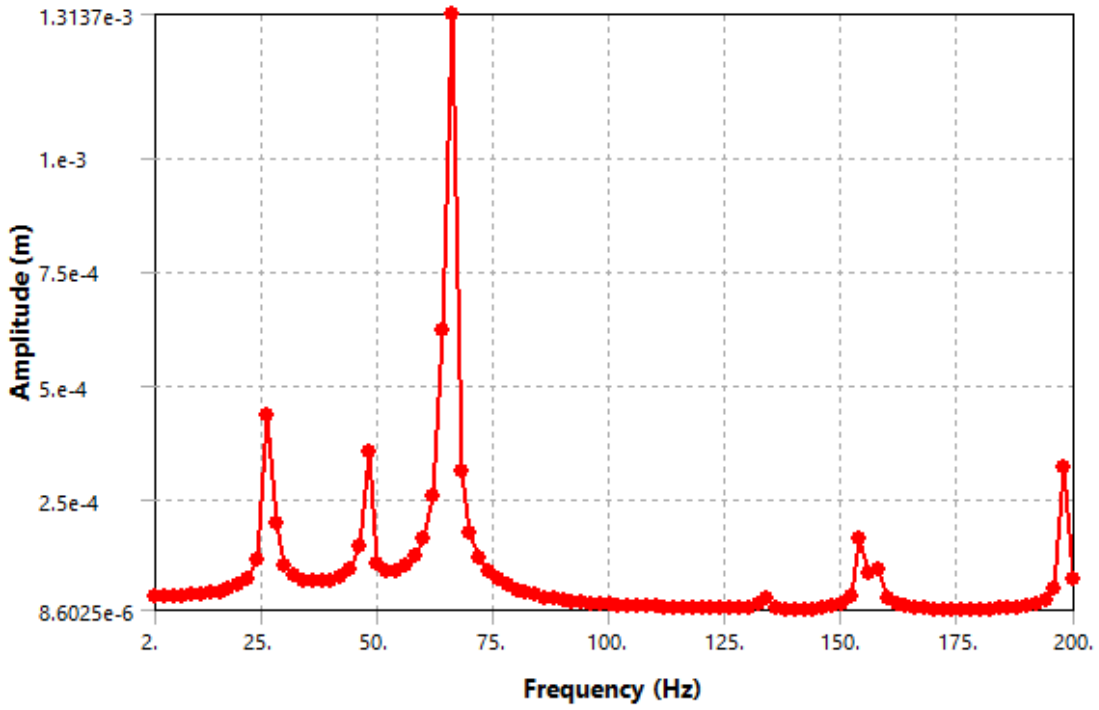

Figure 4.9: Variation of displacement amplitude with different frequencies

It is clear that the maximum peak amplitude was generated at operating frequency of 66

Hz. Other significantly high peaks corresponded to the frequencies 25 Hz, 49 Hz, 153 Hz and 197 Hz as shown in Figure 4.9. From modal analysis, the second, the third, fifth, seventh and ninth natural frequencies of the ball mill structure were 26.6 Hz, 47.6 Hz, 65.4 Hz, 154.5 Hz, and 198.4 Hz respectively. Since the natural frequencies are different from the operating frequency of the ball mill, there was no resonance in the ball mill developed.

4.4.1 Harmonic response results for the ball mill drum

The harmonic response of the ball mill drum with the shaft was calculated. A plot of response of the amplitude versus frequency graph was as shown in Figure 4.10.

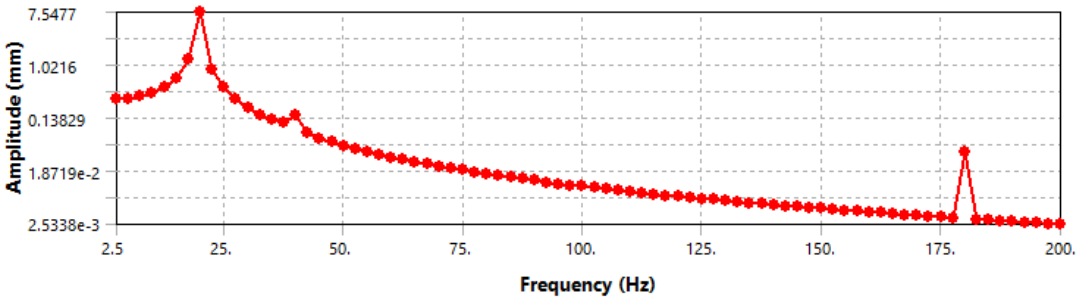

Figure 4.10: Variation of displacement amplitude with different exciting frequencies

Figure 4.10 showed that the maximum amplitude was generated in 20Hz and the corresponding value of amplitude was 7.5477mm. Resonance could occur if the excitation frequency matched with this frequency. This frequency was close to the 4th and 5th order predicted natural frequencies. Therefore, the 4th and 5th modes shapes were the resonance frequencies for ball mill considering the drum and shaft only.

The drum and the shaft were bound to be the most affected since the highest amplitude of the 4th and 5th natural frequencies were located there. Consequently, the structure of the ball mill needs to be optimized in order to enhance the stiffness.

4.5 Parameters influencing the vibration

From modal and harmonic analysis, the 4th, 5th and 6th mode shapes show high twisting when the whole ball is considered when only the drum is considered the 4th 5th modes shapes are the resonance frequency. This explain that the design of the ball mill needs to avoid these natural frequencies. The natural frequency is dictated by mass and stiffness of

the structure, according to Equation 4.1.

$$\omega = \sqrt{\frac{k}{m}}, \tag{4.1}$$

where k is stiffness, and m is mass.

The mass is influenced by the length and diameter of ball mill drum. The stiffness of the structure is influenced by the material selection, the structure and the diameter and the length of the shaft, According to Equation 4.2.

$$k = \frac{G\pi d_2^4}{32L_2}, \tag{4.2}$$

where G is modulus of rigidity of material, d is diameter of shaft, L is length of shaft.

4.6 Transient Analysis

The responses of the ball mill structure due to time dependent load are presented in this section. Vibration amplitude are discussed with respect to the limits and standards of vibration to evaluate whether the vibrations are acceptable. The greater the vibration amplitudes, the higher levels of structure defects (Cornelius Scheffer, 2004).

4.6.1 Acceleration time response

The acceleration time response obtained from ANSYS simulation was as shown in Figure 4.11. The maximum acceleration was $1.41 m/s^2$.

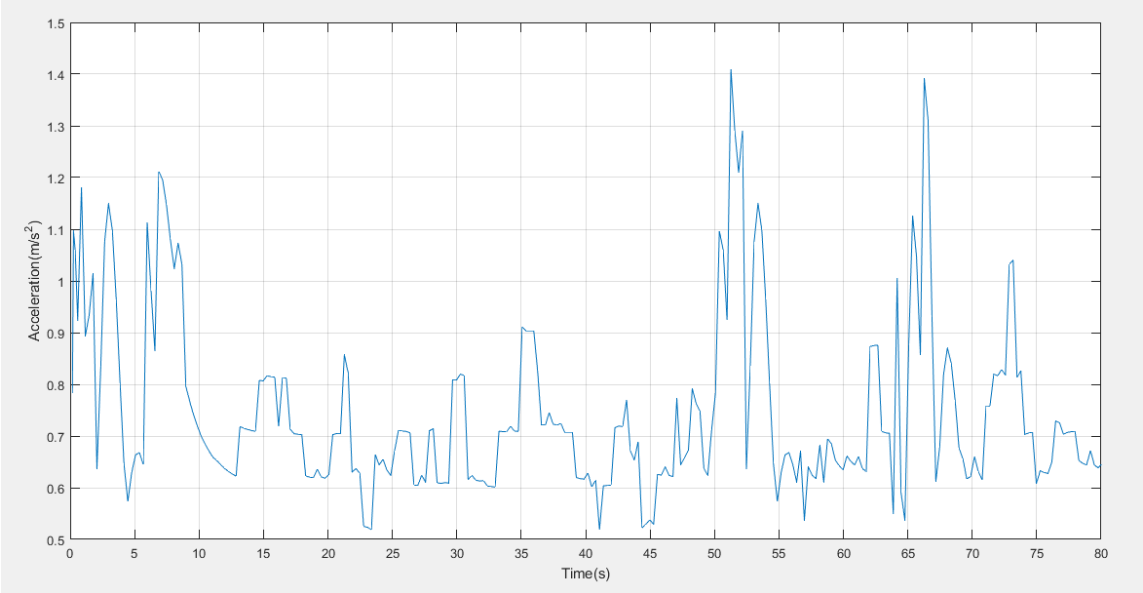

Figure 4.11: Acceleration time response

Figure 4.12 shows the acceleration contour at $t = 80sec$. It was seen that the acceleration increased from bottom of the ball mill structure to the top.

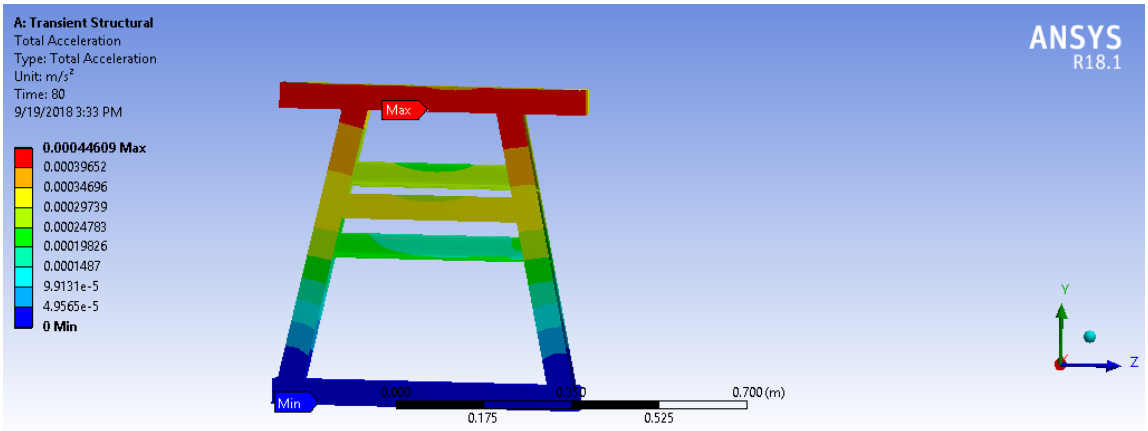

Figure 4.12: Contour of acceleration distribution

The acceleration response was also calculated in the frequency domain by using Fast Fourier Transform (FFT). Figure 4.13 shows the acceleration response in frequency domain. Peak amplitudes of 7.2×10^{-3} mm and 6.6×10^{-3} mm were observed at 0.0 6Hz and 0.14 Hz respectively. It is clear that these frequencies are far below the natural frequencies calculated in modal analysis, and their amplitudes are very low. This confirmed that resonance would not happen.

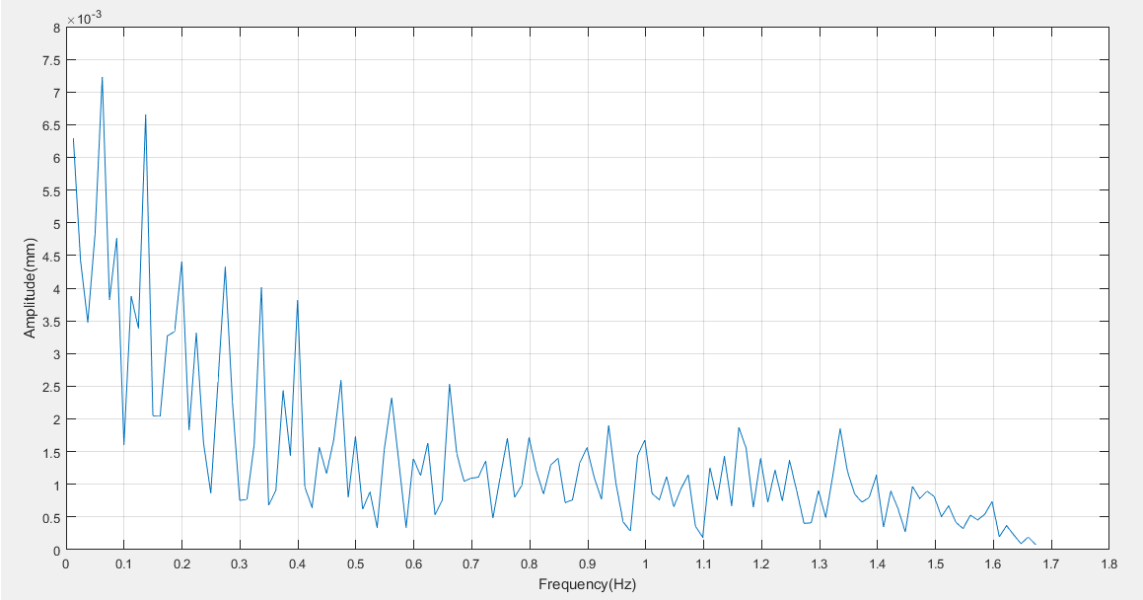

Figure 4.13: Frequency domain of acceleration response

4.6.2 Deformation of the ball mill

Figure 4.14 shows the deformation time response of the ball mill structure during operation of the ball mill. The maximum total deformation observed was 8.95×10^{-5} m and minimum deformation was 0 m.

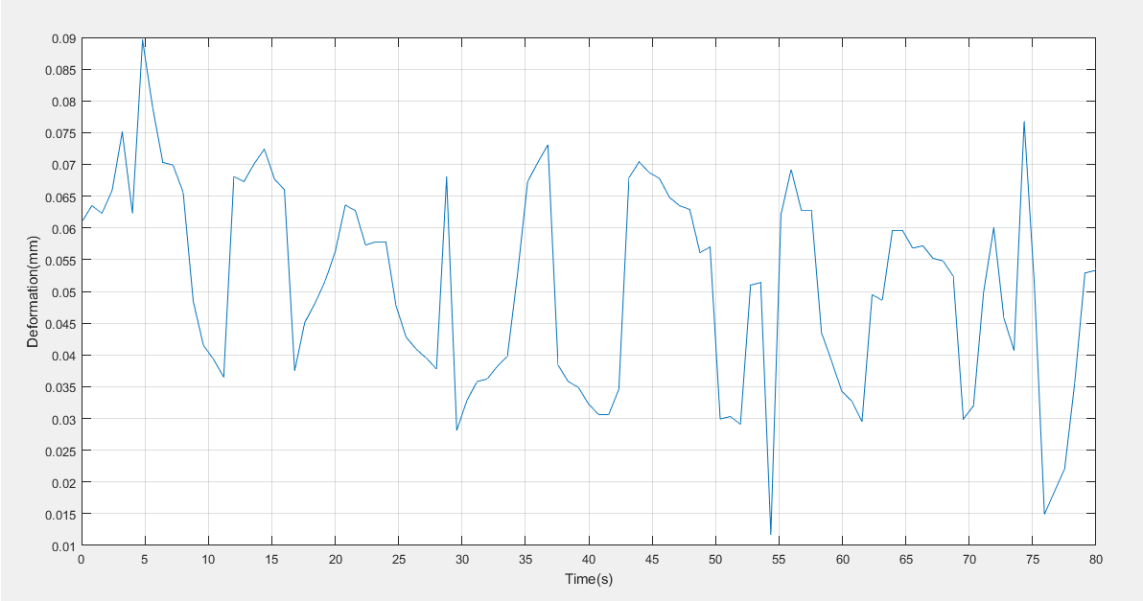

Figure 4.14: Total deformation

Figure 4.15 shows the total deformation at time $t = 80sec$. It is clear that the maximum deformation occurred on the the top member of frame support because it was the contact point between the frame support and the drum. The minimum deformation occurred on the lower member of the frame support. It was found out that the deformation varied with respect to time as the excitation force was a random time varying load. This deformation was little and good for the working condition of the ball mill since it was within the limits of acceptable vibration.

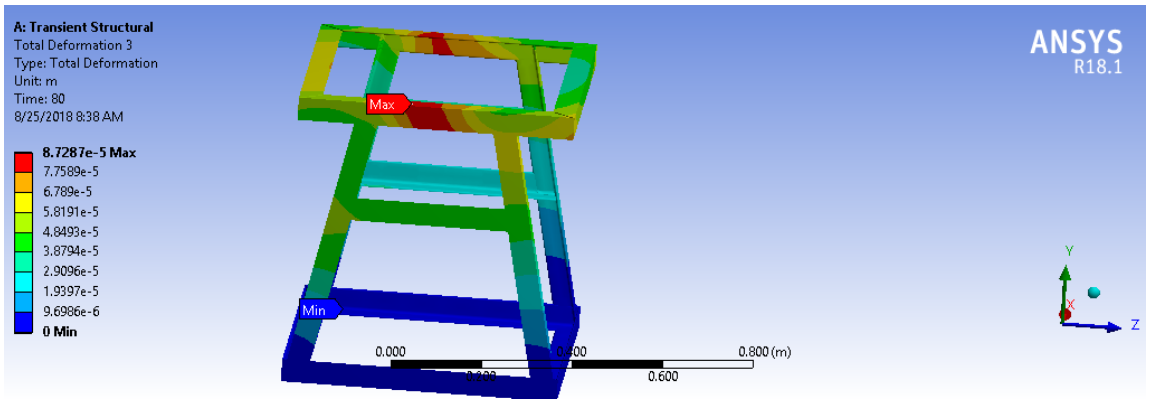

Figure 4.15: Total deformation at 80s.

4.6.3 Stress distribution

Figure 4.16 shows the distribution of stress in the ball mill at $t = 80sec$. It is clear that the highest stress concentration was experienced on top members of the frame support with the maximum stresses being located at the sharp joints as shown in Figure 4.17. This is because it is the upper part of the support that carried the rotating drum and it was where the maximum vibrations were found.

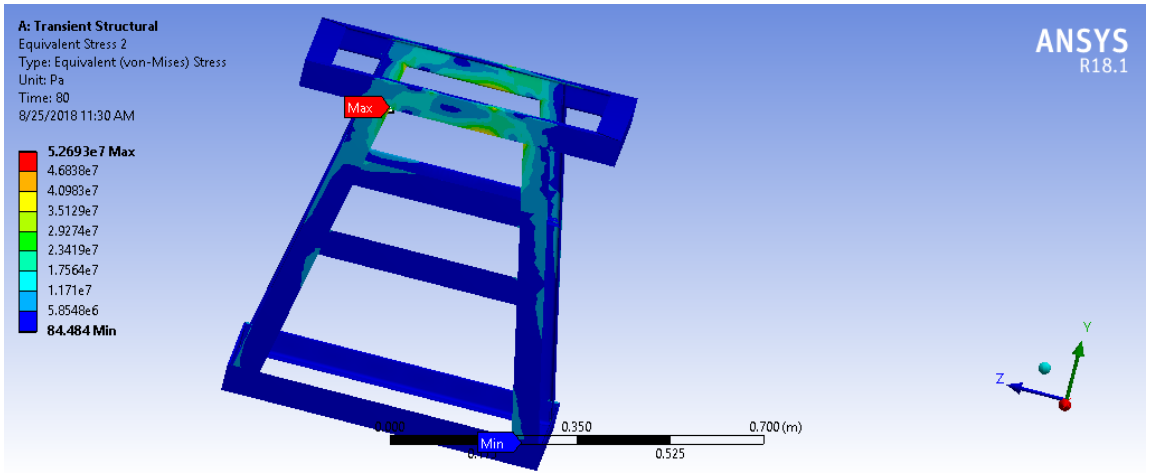

Figure 4.16: Stress distribution at t= 80 seconds

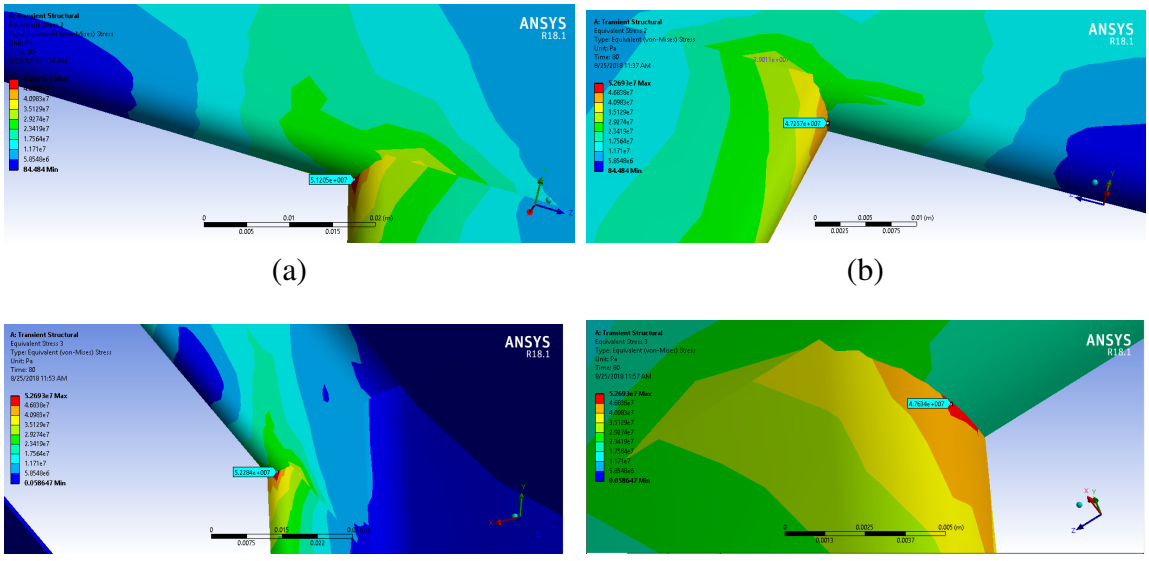

Figure 4.17: Location with highest stress

Figure 4.18 shows the change in stress with time in the ball mill structure. The maximum stress observed was 68.22 MPa.

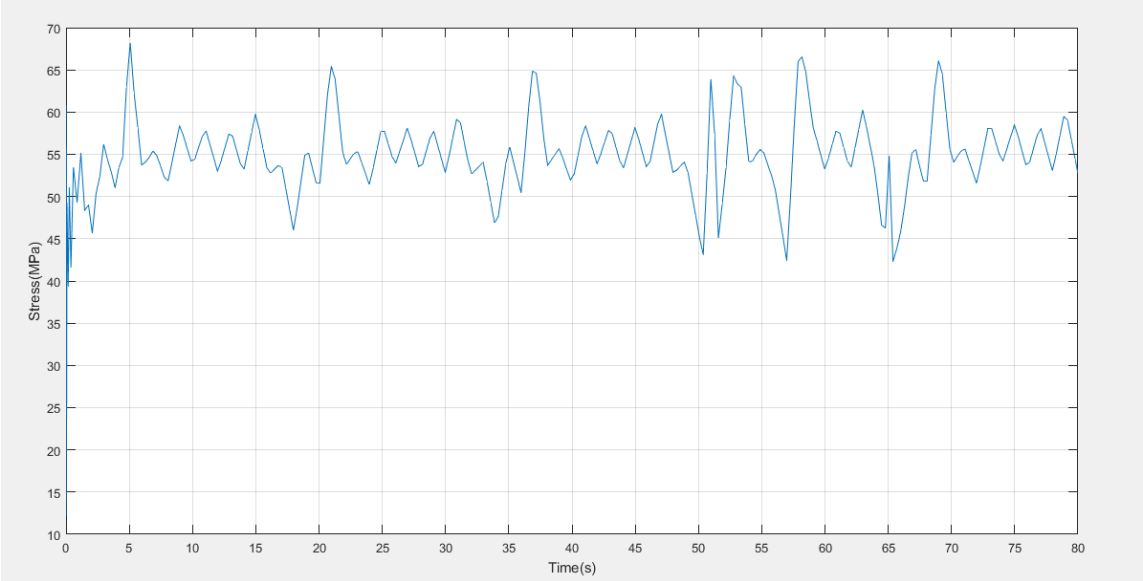

Figure 4.18: Stress response

The yield stress of structural steel which is 250 MPa is much higher than 68.22 MPa stress observed in the ball mill structure thus indicating a factor of safety of 3.6. This showed

that the deformation of the ball mill was still elastic. Therefore, the ball mill structure was safe against the loading from the tumbling of media charge. However, the failure due to fatigue could happen from stress concentration points as shown in Figure 4.17.

4.6.4 Effect of ball mill rotation speed on the vibration

The vibration amplitude was measured in terms of acceleration obtained at different rotation speeds of the ball mill at two locations in order to analyze the effect of ball mill rotation speed. From Figure 4.19, as the ball mill rotation speed increased the vibrations rose until a certain speed where a continued increase in speed caused a reduction in vibrations. This is because at high ball mill speeds, impact forces that were the main cause of vibration of ball mill structure decreased. Vibrations increased almost linearly up to 70% but the maximum value was at 80% of critical speed.

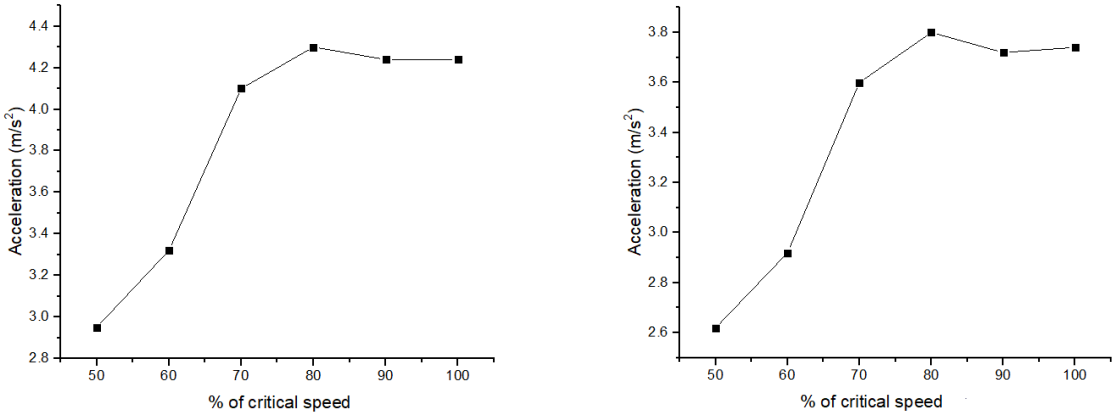

(a) Location A (b) Location B

Figure 4.19: Effect of ball mill speed on vibration

4.7 Experimental results

This section presents the results from experiment. Data obtained from sensor (with a sampling frequency of 1Hz to 10 kHz) are presented here.The acceleration was quantified using root mean square (RMS) since it is the most relevant way of measuring amplitude (Smith, 1989).

The experiment was carried out at two locations as discussed in chapter 3. The following are results obtained for location A and location B.

4.7.1 Location A

The vibration of the ball mill at a rotation speed of 70% of critical speed was as shown in Figure 4.20.

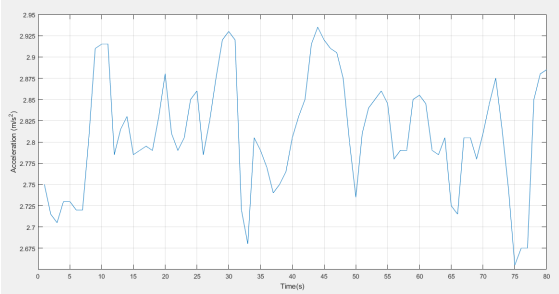

(a) Acceleration in X-direction

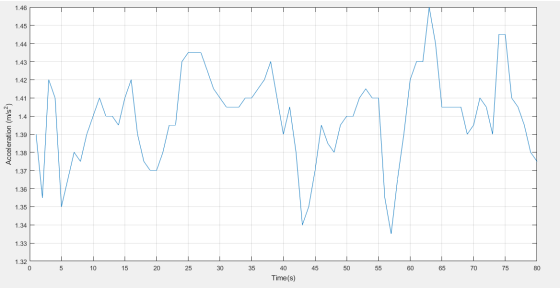

(b) Acceleration in Y-direction

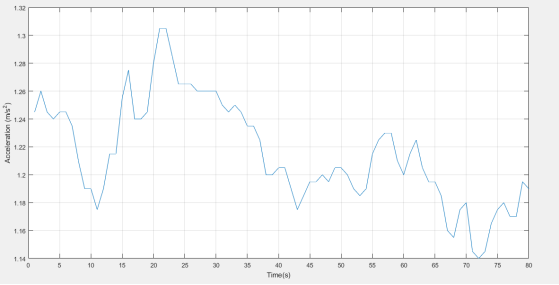

(c) Acceleration in Z-direction

Figure 4.20: Acceleration time history at 70% of critical speed Location A

The acceleration time response in X-direction, Y-direction, Z-direction were as shown in Figure 4.20a, Figure4.20b,and Figure4.20c respectively. The maximum amplitude of acceleration was observed to be the highest in the X-direction and least in Z-direction. This is because the drum rotates along the Y-axis, i.e. moves in the X-Z plane and therefore higher vibrations are expected in this plane. However, vibrations in the Z-axis are absorbed by the frame thus most of the vibrations will be in the X-axis. The vibrations in the Y-direction are due to the gear box and the motor.

4.7.2 Location B

The vibration time response of the ball mill at a rotation speed of 70%, measured at location B was as shown in Figure 4.21. Figure 4.21a, 4.21b and 4.21c show the vibration in X, Y and Z-direction respectively. The highest values were observed in the X-direction. This is because as the drum rotate along the Y-axis, it moves in the X-Z plane and therefore higher vibrations are expected in this plane. However, vibrations in the Z-axis are

absorbed by the frame. The vibrations in the Y-direction are due to the gear box and the motor.

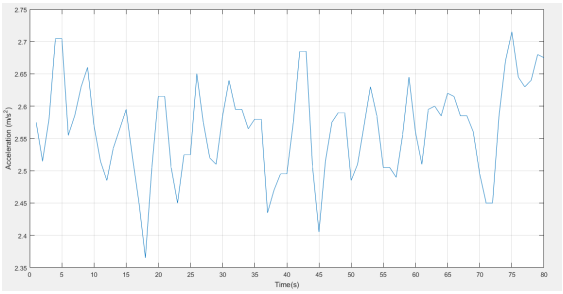

(a) Acceleration in X-direction

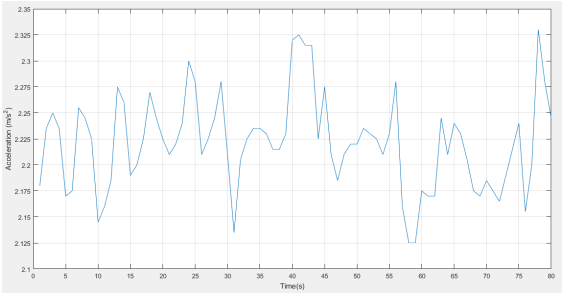

(b) Acceleration in Y-direction

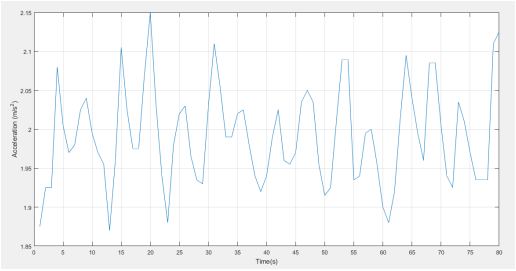

(c) Acceleration in Z-direction

Figure 4.21: Acceleration time history at 70% of critical speed Location B

4.7.3 Effect of drum rotation speed on the vibration

The effect of ball mill rotation speed on the vibration was investigated on different rotation speed shown in Table 4.2. The results for location A and B are presented in this section.

Table 4.2: Rotations speed

Rotation speed (rpm)	% of critical speed
35	50
42	60
49	70
56	80
63	90
70	100

Variation of vibration with ball mill rotation speed at location A was as shown in Figure 4.22. It is seen that vibrations increased as the ball mill rotation speed increased until a certain value of speed where vibrations started decreasing. This is because at low speed there was cascading and the balls rolled over each other without falling to the bottom thus the impact forces were low. However, an increase in speed resulted in cataracting whereby individual balls were thrown clear of the mass and fall on the drum with higher impact forces and thus higher vibrations. Nevertheless, when the critical rotation speed was reached, centrifuging occurred and the balls did not fall since the centrifugal forces were equal to the centripetal forces.

The lack of falling materials resulted in reduced impact forces. Figure 4.22a shows directional vibrations. Vibrations in X-direction were high, whereas vibrations in Z-direction were the least. This is because Z-direction was in direction of the shaft and other directions were in the direction of rotation of ball mill.

Figure 4.22b shows the total vibration of a ball mill at different ball mill rotation speed for location A. Vibrations increased linearly with increase in ball mill rotation speed until 70% of critical speed.

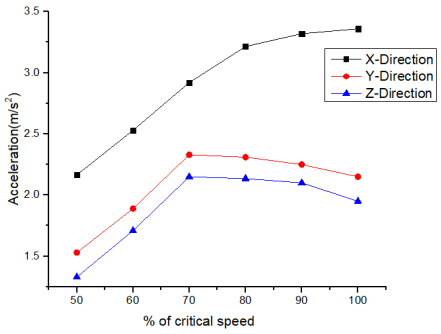

(a) Directional vibration

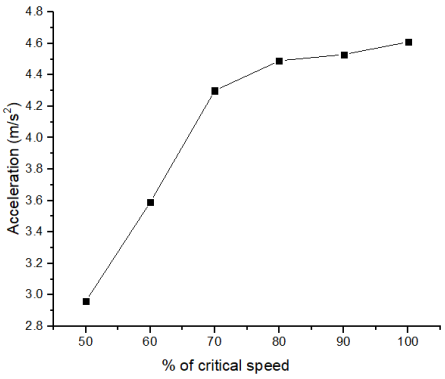

(b) Total vibration

Figure 4.22: Effect of ball mill speed on vibration

Vibration at location B were shown in Figure 4.23. Vibrations increased as the ball mill rotation speed increased, but at 70% to 80% of critical speed, the vibration started decreasing slightly in Z and Y direction as shown in Figure 4.23a. However, in the X-direction, vibrations continued increasing but by a small amount. It was seen also that vibrations in X-direction were higher compared to other directions. This is because X-direction was the direction of the rotation of the ball mill.

Figure 4.23b shows the total vibrations at location B. Vibration increased linearly with increase in the ball mill rotation speed until 70%. This can be attributed to the increase of impact loads with the rotation speed as the motion of balls changed from cascading to cataracting .

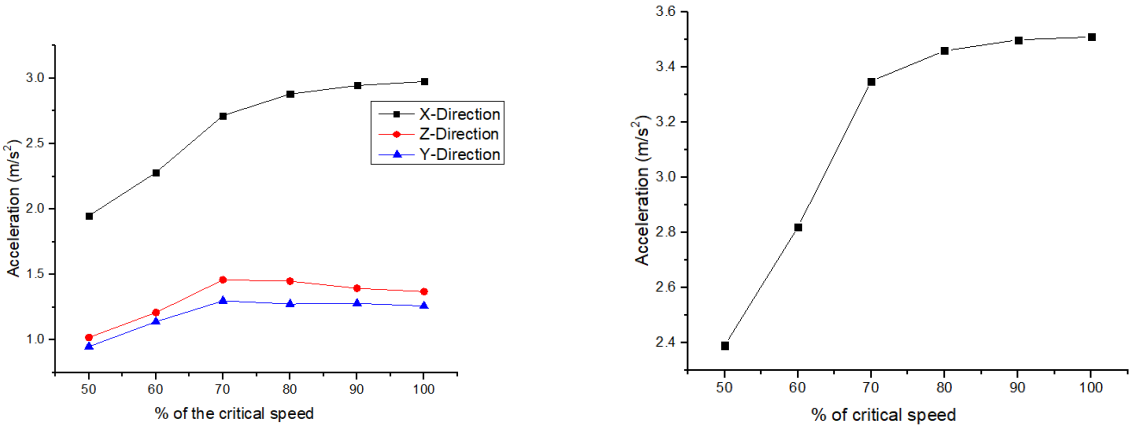

(a) Directional vibration (b) Total vibration

Figure 4.23: Effect of ball mill speed on vibration

Vibration amplitude for both locations increased linearly with ball mill rotation speed until 70% of critical speed where vibration is 4.3 m/s^2 and 3.35 m/s^2 for location A and B respectively. The rotation speed of the ball mill influenced the vibration of structural parts of a ball mill. Experimental work showed that at both locations, the vibration in X-direction was higher compared to the other directions. This was similar to the modal analysis where modes in X direction showed high amplitude. This was because as the drum rotated along the Y-axis, it moved in the X-Z plane and therefore higher vibrations were expected in this plane. However, vibrations in the Z-axis were absorbed by the frame.

CHAPTER FIVE
CONCLUSION AND RECOMMENDATIONS

5.1 Conclusion

An analysis of the vibration problem has been presented in this research work. The analysis involved DEM analysis of the media inside the drum using EDEM software, and FEA of the response of the ball mill structure using ANSYS software. Based on the outcome of this research the following conclusions were drawn:

(a) The fundamental natural frequency was 7.02 Hz, it was higher than operating frequencies of the ball mill 2.4 Hz from the impact load. Hence, the ball mill was not likely to resonance condition during operation. However, The stiffness of the structure and the speed of the ball mill were shown to influence the vibration of the ball mill. The stiffness of the structure is not enough, this can be increased by adding side braces and by increasing the diameter of the shaft.

(b) From harmonic response analysis, it was found that there were 5 peaks amplitudes. The corresponding frequencies are: 25Hz, 49Hz, 66Hz, 153Hz and 197Hz. These frequencies were way above the operating frequencies of the ball mill. Therefore, it was confirmed also that the ball mill structure was safe against resonance conditions. However, the peak amplitudes are bit high which shows that the design is not optimal.

(c) The maximum stress value was 68.22 Mpa, it was located in the top member of the frame support. At this region the stress achieves about 27.3% of yield stress the ball mill structure material (250 MPa), with a factor of safety of 3.6, which shows that the strength of the ball mill structure will not be affected. However,stress concentration need to be reduced by redesigning joints in order to avoid fatigue failure.

5.2 Recommendations

From this research work, the following recommendations were outlined for further study:

(a) Optimization of the structure should be done in order to reduce the stress concentration in some location.

(b) Effect of lifters configurations on the vibration should be investigated.

(c) Ball size and numbers should be varied in order to investigate their effect on the vibration of the ball mill.

References

Ahmed, S., A. (1991). *Theory of vibration: An introduction* (Vol. Volume I; L. Frederick F., Ed.). New York: Springer-Verlag.

ANSYS. (2017). *Mechanical user ' s guide 18*.

Ansys mechanical, harmonic response [Computer software manual]. (2009, July).

Ansys mechanical, modal analysis [Computer software manual]. (2009, July).

Ansys meshing advanced techniques [Computer software manual]. (2017, April).

Barreto, D. M. L. (2018). *Economic contributions of artisanal and small-scale mining in kenya : Gold and gemstones.*

Bathe, K.-J. (2016). *Finite element procedures* (Second ed.). Printice Hall, Pearson Education, Inc.

Chen, L., Xue, Y., Liu, Y., & Li, J. (2014). Modal analysis of oversize ball mill tube based on ANSYS. *Advanced Materials Research*, *889-890*, 62–65. doi: 10.4028/www.scientific.net/AMR.889-890.62

Cleary, P. (1998). Predicting charge motion, Power Draw , Segragation and Wear in Ball Mills Using Discrete Element Methods. *Minerals Engineering*, *11(11)*(February), 1061–1080.

Cornelius Scheffer, P. G. (2004). *Practical machinery vibration analysis and predictive maintenance* (1st ed.). Newnes.

Djordjevic, N., Shi, F., & Morrison, R. (2004). Determination of lifter design, speed and filling effects in ag mills by 3d dem. *Minerals Engineering*, 1135-1142.

Edem 2.4 user guide [Computer software manual]. (2011). United Kingdom.

Erke Wang, T. N. (2002). Structural dynamic capabilities of ansys. In *Ansys 2002 conference.* Munich, Germany.

Francisco, P., Joaqu N., Manuel, M., aguado Juan, M., & d Juan, C. (2018). Frequency domain characterization of torque in tumbling ball mills using dem modelling : Application to fi lling level monitoring. *Powder Technology*.

Fuerstenau, M. C., & Han, K. N. (2003). *Principles of mineral processing*. Society for Mining Metallurgy and Explorations, Inc.

Han, C., & Guevara, F. (2013). Dynamic Analysis For Ball Mill Foundation. *11th International Conference*.

Hao, F., Yong-jun, Z., & Xiao-ping, W. (2016). Dynamic Characteristics Analysis and Structure Optimization Study of Glaze Spraying Manipulator. , *02005*.

Harvey, P., & for Metals, A. S. (1982). *Engineering properties of steel*. American Society for Metals. Retrieved from `https://books.google.rw/books?id=_oRUAAAAMAAJ`

He, J., & Fu, Z. (2001). *Modal analysis*. Butterworth-Heinemann.

Hentschel, T., Hruschka, F., & Priester, M. (2003). *Artisanal and Mining Artisanal and Small-Scale Mining*. London.

James, M. L., Smith, G. M., Wolford, J. C., & Whaley, P. W. (1994). *Vibration of mechanical and structural systems* (second ed.). Harper Collins College.

Jian Tang, Z. W., & Liu, Z. (2016). Ball Mill Shell Vibration Signal Analysis Strategy

Based on DEM-FEM Method and Multi-Component Signal Adaptive Decomposition Technique. , 293–297.

Jiang, S., Ye, Y., Tan, Y., Liu, S., Liu, J., Zhang, H., & Yang, D. (2018). Discrete element simulation of particle motion in ball mills based on similarity Discrete element simulation of particle motion in ball mills based on similarity. *Powder Technology*, *335*(June). Retrieved from `https://doi.org/10.1016/j.powtec.2018.05.012` doi: 10.1016/j.powtec.2018.05.012

Jonsen, P., Bertil, P., & Haggblad, H. (2011). Modelling of internal stresses in grinding charges. In *Ii international conference on particle-based methods fundamentals and applications.*

Jonsén, P., Stener, J., I.Palsson, B., & Hans-Ake, H. (2013). Validation of Tumbling Mill Charge Induced Torque as Predicted by Simulations. *SME Annual Meeting*, 1–6.

Jons P., Pson, B., Tano, K., & Berggren, A. (2011). Prediction of mill structure behaviour in a tumbling mill. *Mineral Engeneering*, *24*, 236-244.

Joseph, W. T., William, G. M., & Allen, C. (1999). *Structure dynamics: Theory and application* (1st, Ed.). Prentice-Hall.

Kalemtas, A. (2013). *Ceramic mater.*

King, R. P. (2001). *Modeling and simulation of mineral processing systems*. University of Utah, USA: Butterworh-Heinemann.

Kulya, C. (2008). *Using discrete element modelling (dem) and breakage experiments to model the comminution action in a tumbling mill* (Unpublished master's thesis).

University of Cape Town.

Lee, H. (2018). *Finite element simulations with ansys workbench 18*. SDC Publications. Retrieved from https://books.google.co.ke/books?id=LdNTDwAAQBAJ

Li, T. Q., Peng, Y. X., Zhu, Z. C., Zou, S. Y., Chang, X. D., & Chen, G. A. (2015). Energy dissipation during the impact of steel ball with liner in a tumbling ball mill. *Material research innovations*, *19*. doi: 10.1179/1432891715Z.0000000001452

Li, W., Pu, H., Liu, Q., Chen, G., & Zhang, S. (2009). ANSYS-Based Dynamic Analysis of High-Speed Motorized Spindle. In *2009 international conference on computer engineering and technology*. doi: 10.1109/ICCET.2009.41

Liu, Z. (2008). The analysis of vibro-acoustic coupled characteristics of ball mill cylinder under impact excitation. *Modern Applied Science*.

Martins, S. (2011). *Exploring tumbling mill dynamics through sensor development* (Unpublished doctoral dissertation). McGill University.

Mayur, H. P., & Vishal, A. P. (2014). Design and Analysis of Ball Mill For Paint Industries. , *2*(04), 471–476.

Mishra, B., & Rajamani, R. K. (1992). The discrete element method for the simulation of ball mills. *Applied Mathematical Modelling*, *16*(11), 598–604. doi: 10.1016/0307-904X(92)90035-2

Mishra, B. K. (2003). A review of computer simulation of tumbling mills by the discrete element method: Part I-contact mechanics. *International Journal of Mineral Processing*, *71*(1-4), 73–93. doi: 10.1016/S0301-7516(03)00032-2

Moaveni, S. (1999). *Finite element analysis* (B. Stenquist, Ed.). New Jersey: PrentPrentice, Inc.

Morgan, K. (2015). Shock & Vibration using ANSYS Mechanical..

Moveni, S. (2009). *Finit element analysis- theory and application with ansys* (Second ed.). Prentice-Hall.

Olek Zienkiewicz, J. Z., Robert Taylor. (2013). *The finite element method: its basics and fundamentals*. Butterworth-Heinemann.

Palsson, I., & Jonsén, P. (2009). Prediction of contact forces between a grinding charge and mill lifter. In *12th european symposium on comminution and classification escc.*

Petrakis, E., Stamboliadis, E., & Komnitsas, K. (2017). Identification of optimal mill operating parameters during grinding of quartz with the use of population balance modeling. *KONA Powder and Particle Journal*, *2017*(34), 213–223. doi: 10.14356/kona.2017007

Porto, T., Carvalho, L., & Mendonca, B. (2012). Basic Design Requirements for Structures Subjected to Dynamic action. *Argentine Association For Computational Mechanics (AMCA)*, *XXXI*, 2547–2560.

Powell, M., Weerasekara, N., Cole, S., LaRoche, R., & Favier, J. (2011). Demmodelling of liner evolution and its influence on grinding rate in ball mills. *Minerals Engineering*, *24*, 341351.

Quan, Y. (2006). *Finite element analysis of tumbling mill design and operating effects on liner bolt stresses, liner stresses and mill resonance* (Maters, McGill). doi: 10.1177/

001088048002100210

Radziszewski, P., Quan, Y. Y., & Poirier, J. (2017). Design Parameters affecting Tumbling mill natural Frequencies. In *Canadian engineering education association (ceea).*

Rahmanovic, S., Lukavac, C. P., Isic, S., & Mostar, M. F. (2008). An Experimental analysis of Vibration of a ball mill with variable load. In *Twelfth international research/expert conference* (pp. 945–948).

Rao, S. S. (2010). *Mechanical vibrations* (Fifth ed.; M. J. Horton & T. Quinn, Eds.). University of Miami: Prentice Hall.

Rusinski, E., Czmochowski, J., Iluk, A., & Kowalczyk, M. (2010). An analysis of the causes of a bwe counterweight boom support fracture. *Engineering Failure Analysis,*, *17*, 179-191.

Rusinski, E., Dragan, S., Moczko, P., & Pietrusiak, D. (2012). Implementation of experimental method of determining modal characteristics of surface mining machinery in the modernization of the excavating unit. *Archives of Civil and Mechanical Engineering*, *12*, 471-476.

Rusiński, E., Moczko, P., Pietrusiak, D., & Przybyłek, G. (2013). Experimental and numerical studies of jaw crusher supporting structure fatigue failure. *Strojniski Vestnik/Journal of Mechanical Engineering*, *59*(9), 556–563. doi: 10.5545/sv-jme.2012.940

Seccatore, J., Veiga, M., Origliasso, C., Marin, T., & Tomi, G. D. (2014). An estimation of the artisanal small-scale production of gold in the world. *Science of the Total*

Environment.

Sheng-yong, L., Qiong-jing, M., Zheng, P., Xiao-Dong, L., & Jian-Hua, Y. (2012). Simulation of ball motion and energy transfer in a planetary ball mill. *Chin. Phys. B*, *21*(7), 1–9. doi: 10.1088/1674-1056/21/7/078201

Smith, J. D. (1989). *Vibration measurement and analysis*. London: Butterworh & Co.

Tang, J., Wu, Z., & Liu, Z. (2016). Ball Mill Shell Vibration Signal Analysis Strategy Based on DEM-FEM Method and Multi-Component Signal Adaptive Decomposition Technique. *International Forum on Management, Education and Information Technology*(Ifmeita), 293–297.

Toram, K. K. (2005). *Grinding media oscillation: Effect on torsional vibrations in tumble mills* (Unpublished master's thesis). Texas A&M University.

Venugopal, R., & Rajamani, R. K. (2001). 3D simulation of charge motion in tumbling mills by the discrete element method. *Powder Technology*, 157–166.

Wassgren, C., & Sarkar, A. (2008). Discrete element method (dem) course module. *https://pharmahub.org/resources/113*.

Weerasekara, N. S., Powell, M. S., Cleary, P. W., Tavares, L. M., Evertsson, M., Morrison, R. D., ... Carvalho, R. M. (2013). The contribution of DEM to the science of comminution. *Powder Technology*, *248*, 3–24. doi: 10.1016/j.powtec.2013.05.032

Wills, B. A., & Napier-munn, T. (2006). *An Introduction to the Practical Aspects of Ore Treatment and Mineral Recovery* (7th ed.). Elsevier Science & technology Books.

Wojcicki, Z., Grosel, J., Sawicki, W., & Majcher, K. (2015). Experimental (oma) and

numerical (fem) modal analysis of ball mill foundations. *Procedia Engineering*.

Yang, D., Yu, Z., Zhang, L., & Cheng, W. (2017). Modal Analysis of Automobile Brake Drum Based on ANSYS Workbench. *Advanced in Computer Science Research*, *75*.

Yu, Y., Zhang, S., Li, H., Wang, X., & Tang, Y. (2017). Modal and harmonic response analysis of key components of ditch device based on ansys. *Elsevier (Procedia Engineering)*.

Zeng, Y., & Forssberg, E. (1992). Effects of operating parameters on vibration signal under laboratory scale ball grinding conditions. , *35*, 273–290.

APPENDICES

Appendix I: Main parts of the ball mill developed in JKUAT

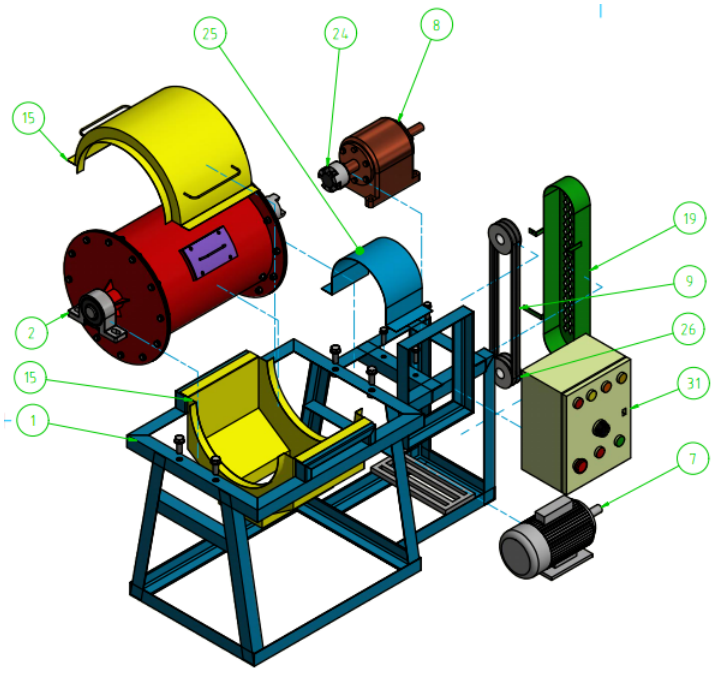

Parts List			
ITEM	PART NUMBER	QTY	DESCRIPTION
1	Ball mill Frame	1	Equal Leg Channels 50x50x4
2	Pillow block Bearing	2	UPC 210, 50 MM BORE
7	Electric motor	1	4KW, 3 Phase, 50Hz
8	Gear Box	1	Inline Shaft, Helical Gear
9	V-Belt	2	Class A
15	Dust Hood	1	Top and Bottom Cover
19	Guard 1	1	Protecting Pulley - Belt system
24	Jaw Coupling Assembly	1	L100 Series
25	Guard coupling	1	Protecting Coupling section
26	Pulley	2	Double groove
31	Motor Control Centre	1	ON-OFF Switches, VFD, Motor Protection, Timer, Emergency Switch, Indicators

Parts of ball mill developed in JKUAT

Appendix II: CAD model of the ball mill developed in JKUAT

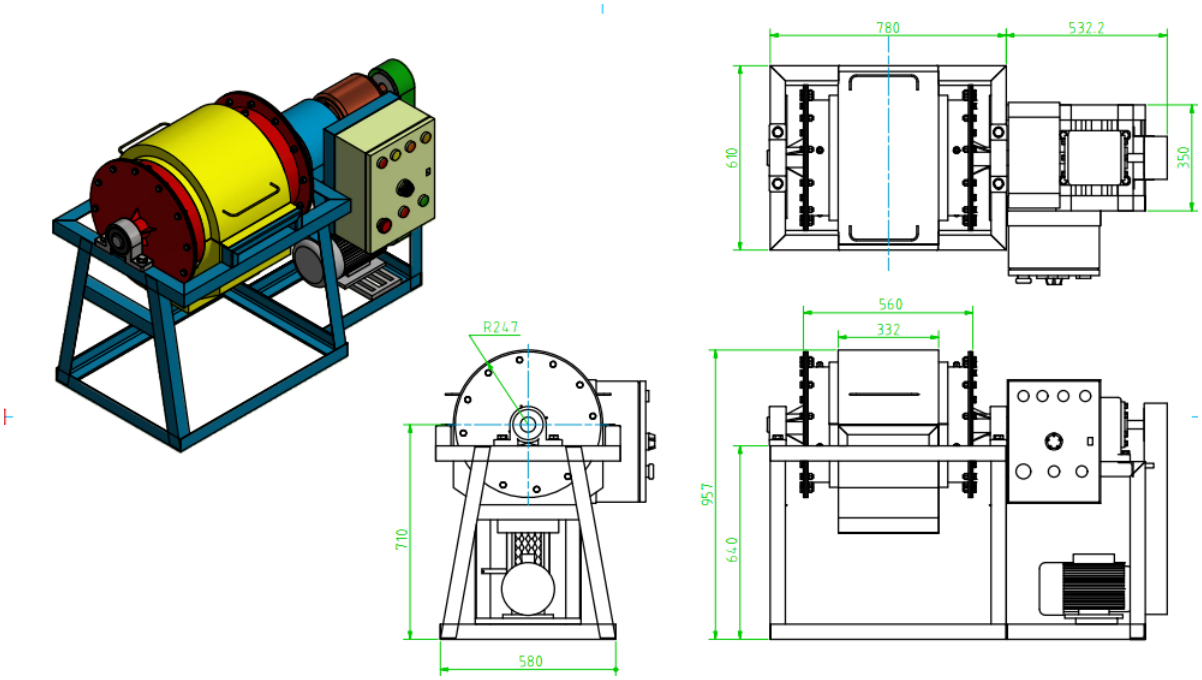

Model of ball mill developed in JKUAT

Appendix III: Convergence for transient analysis

The transient simulation solver output for the last cumulative iteration, which shows that the simulation has converged is shown below. As shown for the last sub-step which is 6450, the force convergence is 0.1497×10^{-1} and the force criterion is 9.409.

```
   DISP CONVERGENCE VALUE   =  0.4979E-04  CRITERION=  0.3639E-05
   LINE SEARCH PARAMETER =  0.9989     SCALED MAX DOF INC = -0.2620E-03
   FORCE CONVERGENCE VALUE  =   634.3      CRITERION=   9.225
  EQUIL ITER   2 COMPLETED.  NEW TRIANG MATRIX.  MAX DOF INC= -0.3137E-06
   DISP CONVERGENCE VALUE   =  0.6153E-07  CRITERION=  0.3713E-05 <<< CONVERGED
   LINE SEARCH PARAMETER =   1.000     SCALED MAX DOF INC = -0.3137E-06
   FORCE CONVERGENCE VALUE  =  0.3353E-01  CRITERION=   9.413     <<< CONVERGED
  >>> SOLUTION CONVERGED AFTER EQUILIBRIUM ITERATION   2
*** LOAD STEP     1   SUBSTEP  3203  COMPLETED.    CUM ITER =   6448
*** TIME =   15.9964         TIME INC =  0.500000E-02
*** RESPONSE FREQ =  1.505       PERIOD=  0.6646      PTS/CYC = 0.13E+03
*** AUTO TIME STEP:  NEXT TIME INC = 0.36500E-02  DECREASED (FACTOR = 0.7300)

   FORCE CONVERGENCE VALUE  =   230.1      CRITERION=   9.039
   DISP CONVERGENCE VALUE   =  0.3639E-04  CRITERION=  0.3566E-05
  EQUIL ITER   1 COMPLETED.  NEW TRIANG MATRIX.  MAX DOF INC= -0.1915E-03
   DISP CONVERGENCE VALUE   =  0.3638E-04  CRITERION=  0.3639E-05
   LINE SEARCH PARAMETER =  0.9997     SCALED MAX DOF INC = -0.1914E-03
   FORCE CONVERGENCE VALUE  =   338.5      CRITERION=   9.221
  EQUIL ITER   2 COMPLETED.  NEW TRIANG MATRIX.  MAX DOF INC= -0.6400E-07
   DISP CONVERGENCE VALUE   =  0.1348E-07  CRITERION=  0.3713E-05 <<< CONVERGED
   LINE SEARCH PARAMETER =   1.000     SCALED MAX DOF INC = -0.6400E-07
   FORCE CONVERGENCE VALUE  =  0.1497E-01  CRITERION=   9.409     <<< CONVERGED
  >>> SOLUTION CONVERGED AFTER EQUILIBRIUM ITERATION   2
```

Last cumulative iteration